PNC-TN9410 87-088 Tr

[redacted]

[redacted]

[redacted]

LARGE-SCALE TEST ON SODIUM LEAK AND FIRE(IV)

—Test of Sodium Leak and Fire Using Simulated Piping ; Run-E2—

[redacted]

June, 1987

OARAI ENGINEERING CENTER

POWER REACTOR AND NUCLEAR FUEL DEVELOPMENT CORPORATION

PNC-TN9410 87-088 Tr

1987年 6 月

大規模ナトリウム漏洩燃焼試験（Ⅳ）

－実機縮尺模擬ナトリウム配管構造体を使用した漏洩燃焼試験，Run-E1－

森井　正*・福地　平*・山田敏夫*・姫野嘉昭*

要　　旨

〔目的〕より現実的な配管からのナトリウム漏洩形態とそれに伴うナトリウム燃焼を明らかにする。

〔方法〕「もんじゅ」二次主冷却系配管の1/3.5縮尺試験体をサファイア施設の鋼製密閉容器SOLFA－2に組み込み，ナトリウム圧力3.8 kg/cm^{2}Gを加えて，その時のナトリウム漏洩形態を観測し，また漏洩に伴う燃焼発熱量の測定を行う。なお，試験体の配管は水平に設置し，漏洩孔はその上部に開口した。漏洩孔の断面積は，実機配管の1/4 Dtを（1/3.5）^{2}に縮尺したもので，また配管周囲には実機と同様に保温構造を取りつけた。試験条件は，ナトリウム温度505℃，漏洩流量3.1 kg/sec，漏洩時間は13分である。

〔結果〕配管周囲の保温構造は，漏洩時のナトリウム流動圧および漏洩ナトリウムの燃焼熱に起因する高温によっても損傷することなく，漏洩ナトリウムがスプレー状となって飛散することを防止する機能を発揮した。漏洩形態は，このため棒状であった。また，漏洩時の燃焼速度は，漏洩ナトリウム流量の約4％であり，前回のスプレー・ノズルを使用したスプレー燃焼試験の対応する値が約30％であったことを考慮すると，保温構造によって燃焼がより穏やかになることが明らかにされた。

〔結論〕配管からの漏洩形態は，従来想定していたようなスプレーではなく，より穏やかな棒状流で，このため漏洩時の燃焼速度もスプレー燃焼の約1/7に過ぎない。

＊　プラント安全工学室，安全工学部

PNC-TN9410 87-088 Tr

June, 1987

Large-Scale Test on Sodium Leak and Fire (Ⅳ)

—— Test of Sodium Leak and Fire Using Simulated Piping ; Run-E2 ——

T. Morii*, T. Fukuchi*, T. Yamada* and Y. Himeno*

Abstract

A test, Run-E2, of sodium leak from a 1/3.5 scale simulated Na piping of the secondary circuit of Monju was conducted using the SOLFA-2 in the SAPFIRE facilities. In the simulated piping, a leak hole with an area reduced by $(1/3.5)^2$ from an area of 1/4·Dt of the actual piping was made on the upper wall of the piping in advance. In the test, a pressure equal to the system pressure of 3.8 $kg/cm^2 \cdot g$ of the hot leg piping in secondary circuit of the actual plant was applied, and sodium was spilled. Spill duration was approximately 13 minutes.

The test results showed that the integrity of the insulation structure around the piping will not be broken by a Na pressure and combustion heat during an accident, therefore, the spray leakage of Na can be fully prevented. Moreover, burning rate of Na during leakage was approximately 4% of the flow rate of the Na leak. Compared to about 30% obtained from the spray combustion test conducted previously using a spray nozzle, the combustion following a realistic Na leak from the actual piping is found to be milder than that of spray combustion.

---

* Plant Safety Engineering Section, Safety Engineering Division.

CONTENTS

LIST OF TABLES

LIST OF FIGURES

1. INTRODUCTION

For the prototype reactor Monju, a Na spray combustion due to a Na leak accident from a leak hole with an area equivalent to 1/4 Dt of piping was postulated as one of the design basis accident. However, the Na piping of the actual plant is surrounded by the insulation which is expected to prevent the spray-type leak of Na during the Na leak accident. To clarify this kind of function, it is necessary to substantiate that the insulation around the piping will not be destroyed by high-temperature Na leaking with the operational system pressure. Therefore, the Na leak test was conducted using a simulated piping with a reduced scale whose insulation structure was the same as the actual piping.

In the present report, the test facility is explained in Chapter 2, test conditions and methods in Chapter 3, test results in Chapter 4, and conclusions in Chapter 5.

2. TEST FACILITIES

The test was conducted using the large-scale sodium leak and combustion test facility (SAPFIRE) in the Plant Safety Engineering Section in the Safety Engineering Division. The SAPFIRE facility comprises SOLFA-1, SOLFA-2, a Na storage and supply system, and a large-scale aerosol and waste liquid treatment system. The present test was conducted in SOLFA-2.

Since the details of the relevant facility were already reported in a previous report¹⁾, only the outline of the facility and the modified portion of the test rig will be explained below.

Figure 2.1 shows a flow sheet diagram of SAPFIRE facility, and Fig. 2.2 shows a section of SOLFA-2.

2.1 SOLFA-2

As shown in Fig. 2.2, SOLFA-2 comprises a main body of test vessel with an oxygen gas supply header, a water cooling jacket around the vessel, a Na catch pan at the bottom of the vessel, a Na drain pipe attached to the Na catch pan, and the simulated sodium pipe with insulation cover.

(referred to below as "simulated pipe").

The test vessel is a vertical, cylindrical closed vessel made of SUS-304 stainless steel with an inner volume of about 111 m^3. The water cooling jacket surrounding the test vessel prevents an excessive temperature rise of the vessel due to heating during a Na combustion. However, in the present test, the water cooling jacket was not filled with water because not much heat was generated. The Na catch pan is located 2,040 mm below the simulated pipe. It receives and stores the leaked Na. After the test, stored Na is drained to an impurities setting tank through the drain pipe located at the center of the Na catch pan. The oxygen gas supply header is able to supply oxygen gas (about 100% pure) at a constant rate of 300N m^3/min during the Na leak test. For the gas blow-off portion of the oxygen gas supply header, numerous holes are provided in the periphery of the ring-shaped header located along the inner wall of the vessel. These holes are covered with wire mesh to permit a gentle outflow of gas to the surrounding portion. In addition, the test vessel has a rupture disk (rupture setting of 1.71 kg/cm^2) for blowing down gas when the inner pressure exceeds the design pressure (2 kg/cm^2).

2.2 Simulated Sodium Pipe

Though the piping of secondary main cooling system of Monju was made of 22B pipes (SUS-304, Sch 20), adopted for the simulated pipe was 8B (SUS-304, Sch 20) pipe. Its construction is shown in Fig. 2.3.

All the dimensions adopted are the same as those of Monju for the thickness of inner and outer jackets used as the surrounding insulation, the thickness of connecting pipe base, connecting pipe base flange and cover plate, and the sizes of outer jacket joints and machine screws. Therefore, although the linear scale is reduced to 0.39 for 8/22, the structural strength has been increased beyond that of the secondary piping of Monju.

(1) Na leak hole

The cross sectional area of the Na leak hole of the simulated pipe was set to 2.3 cm^2 which was obtained by converting the linear scale ratio of 0.39 of the test specimen into an areal scale ratio. That is

$$15.0\ \mathrm{cm}^2 \times 0.39 \times 0.39 = 2.3\ \mathrm{cm}^2.$$

In the above equation, 15.0 cm^2 corresponds to the postulated leak hole of 1/4 Dt of Monju, and 2.3 cm^2 corresponds to the area of a circle with the diameter of 1.69 cm. The leak hole is located on the upper side of the center of piping.

(2) Others

Construction of clamps, connecting pipes, and spacers was scaled down as much as possible from the piping of Monju in accordance with the linear scale ratio.

(3) Materials

Materials of insulation, piping, and inner and outer jackets are as same as those of actual equipment.
For insulating materials, nuclear reactor class Rock Fine was used for the first layer, and ordinary Rock Fine for the second and third layers.

2.3 Na Catch Pan

The Na catch pan is used to simulate the presence of Monju's floor liner. It is made of ordinary carbon steel, and is 3400(ID) × 456(H) and weights 6 tons.

A drain pipe for draining stored Na is provided at the center of the Na catch pan. This drain pipe is made of SUS-304 of 1B Sch 20.

2.4 Instruments, Measured Items, and Measuring Methods

The instruments are basically the same as those used in RUN-E1$^{1)}$. Figure 2.2 also shows the layout of measuring points. Electrical signals for temperature, pressure, flow, and O_2 concentration are recorded on magnetic tape (MT) by electronic computer (YHP-1000).

Na leak phenomenon from the simulated pipe were photographed by two video camera units and one thermovision unit.

2.4.1 Thermal Behavior of the Simulated Pipe

The thermal behavior of the simulated pipe was measured by thermocouples.

Layout of these thermocouples was determined based on the followings:

(1) To ensure proper control of piping temperature (TE1088).

(2) To measure the temperature of inner and outer jackets to find out whether the inner and outer jackets are thermally destroyed or not (TE1089-1091, TE1094-1100).

(3) To measure the temperature of insulating materials to determine if any reactions occur between Na and insulating materials (TE1092, 1093).

(4) To measure the flow direction of the initial Na leak within the insulation.
From the results of test RUN-B3$^{2)}$, we found that the temperature of the inner jacket becomes the same as that of the leak Na immediately after the start of leak and hardly changes during the leak. Since the leaked Na spreads along the bottom of the inner side of the outer jacket, many thermocouples were placed at the bottom of the outer jacket as shown in Fig. 2.4.

(5) To judge the combustion of inflammable gas and the presence of upward flow of Na (TE1099).

2.4.2 Change in Oxygen Concentration

To measure the change in oxygen concentration with time at the bottom, middle and bottom of the vessel as same as RUN-E1 test$^{1)}$, gas inlets to automatic gas sampling unit, gas chromatograph unit, and oxygen concentration were installed at the locations shown in Fig. 2.2.

2.4.3 Changes in Gas Pressure, Hydrogen Gas Concentration, and Aerosol Concentration

Measuring methods and equipment for these changes were the same as those employed in RUN-E1$^{1)}$.

2.4.4 Thermal Radiation from Simulated Pipe

The results of RUN-B3 test[2)] indicated that the temperature at the surfaces of the outer jacket of the simulated pipe rises to 750°C when Na combustion progresses. At such a high temperature, considerable energy is expected to be radiated from the surfaces of outer jacket. Therefore, to measure this radiation energy, two heat flux meters were installed on the wall of test vessel. The whole surface of one of the heat flux meters was shielded from radiation but that of another was exposed. Height of the heat flux meters were the same as that of the simulated pipe as shown in Fig. 2.2.

2.4.5 Form of Na Leak

Tests previously conducted on the form of leakage from the simulated piping were the water test[3)] using a full-scale mock-up and the Na leak test RUN-B3[2)] using SOFT-1 with a reduced-scale model piping. In the latter test, a cover plate for the heater penetration of the outer jacket dislocated, and a Na leaked from this opening. However, the insulation structure of the simulated pipe used in the present test was slightly improved and, because of this, a leak of Na from the joint of outer jacket was expected as same as the case of previous water test. Thus, it was possible for leaked Na to contact the sidewall of the test vessel depending on the deviation of the joint. Therefore, the following evaluation was made:

According to the results of water test, water droplets traveled 50 cm in horizontal direction when they dropped 20 cm as shown in Fig. 2.5. Therefore, the jet of Na can be assumed to fall while drawing the form of parabola as same as the case of water. Since the present test pipe is 2.1 m high, the jet travelling distance in the horizontal direction can be given by the following equation:

$$\frac{0.2}{(0.5)^2} = \frac{2.1}{\chi^2}, \qquad \chi = 1.6 \text{ m} \qquad \text{(A)}$$

Inside radius of the test vessel of SOLFA-2 is about 2.0 m which exceeds the travel in the horizontal direction. In conclusion, there is no possibility of the Na jet colliding with the SOLFA-2 vessel.

The thermocouples were arranged so that the form of leak can be presumed from the arrangement. Thermocouples were also placed on the walls of vessel to be prepared for the impact of leaked Na splashed from the floor.

In addition to the above, heat resistant video cameras (not used when aerosol density is high) for visualizing the form of leak and a thermovision unit (with narrow visual field) were used.

2.4.6 Other Temperature Measurements

The arrangement of thermocouples (T/C) for measuring the temperature of the vessel wall, gas space described above, and others is basically the same as that of test E1.

3. TEST CONDITION AND METHODS

3.1 Test Conditions

Test conditions will be explained below. The basis for each condition will be stated in the following sections.

Test Conditions:

Temperature of leakeed Na:	505°C
Flow rate of leaked Na:	3.1 kg/sec. (measured value) 3.6 kg/sec. (planned value)
Atmoshpheric conditions:	Air atmosphere, moisture as occurs, room temperature as initial temperature.
Air supply:	Test vessel closed, oxygen was supplied at a constant rate of 85.8 Nm^3/hr during the Na leak.
Na pressure in simulated piping:	3.76 $kg/cm^2 \cdot g$

3.1.1 Na Leak Conditions

Of the Na leak accidents that can be postulated in the secondary cooling circuit of Monju, the accident with the highest temperature of leaked Na is a leak from hot leg piping in the secondary cooling system. The Na pressure in this piping is 3.761 $kg/cm^2 \cdot g$. Therefore, the inner Na pressure of the test pipe was set to 3.761 $kg/cm^2 \cdot g$, and Na temperature was set to 505°C which was equal to that in the hot leg piping of actual plant as stated above.

A cover gas pressure of the Na heater was set to 3.789 $kg/cm^2 \cdot g$ which is equal to the sum of the pressure stated above, pressure loss (0.115 $kg/cm^2 \cdot g$) in Na supply system of the test rig, and Na head pressure (-0.0868 $kg/cm^2 \cdot g$ in an early stage of leaking).

3.1.2 Atmospheric Conditions

Sealed conditions were adopted for the test vessel. Moreover, to continue Na combustion during the test, oxygen gas was supplied from the outside of the vessel at a flow rate of 86.8 Nm^3/hr, which was determined from the results of a pre-test analysis by the ASSCOPS code.

3.1.3 Amount of Leaked Na

The amount of leaked Na was set to approximately 2.4 ton, which made the depth of Na in the Na catch pan half of its height.

3.1.4 Flow Rate of Leaked Na

Since the pressure loss coefficient in the route of leaked Na including leak hole was already known from previous experiments, the flow of leaked Na will be estimated using this coefficient.

Table 1 shows the pressure loss coefficient obtained previously. For the full-scale mock-up pipe, a coefficient of 2.3 to 3.0 was obtained in the pressure range of 2.4 to 6.6 kg/cm^2•g.

However, in test RUN-B3 with SOFT-1 using Na, the coefficient was very large (38.9) because the conditions differred from the water test as explained below.

(1) Supply pressure of Na during test was less than one-tenth of that of the water test.

(2) Because of this, the leak occurred from the joint in outer jacket in water test while the leak in RUN-B3 test occurred from an opening for the heater.

(3) Scale ratio of the simulated pipe to the actual one was 0.27, but the area of opening located in the piping was not equal to 0.27 times the leak hole area of 15 m^2 of actual equipment 1/4 Dt.

Therefore, the data of RUN-B3 were excluded, and 2.5 was used as the pressure loss coefficient of test pipe from Table 1. The predicted flow rate of Na leak was approximately 3.6 kg/sec from the following calculations:

$$W = \sqrt{\frac{2\cdot P\cdot A^2\cdot P}{\eta}} = \sqrt{\frac{2\times 3.761\times 9.804\times 10^4\times (2.3\times 10^{-4})^2\times 832}{2.5}} \qquad \text{(B)}$$

$$= 3.6 \text{ (kg/sec)}$$

3.2 Test Methods

The test was conducted using the automatic sequence of measurement controller (CENTUM) in accordance with the following procedures (refer to flow sheet in Fig. 2.1):

(1) Supplying Na and oxygen gas

- Na in the Na heater is heated to 505°C, and gas pressure in Na heater is increased to and maintained at 3.8 $kg/cm^2 \cdot g$.
- Valve VN-105 is opened 100%.

After the above preparation, VN-108 is opened and Na is allowed to spill from test pipe. At this time, the flow of Na leak is not controlled. Oxygen gas is supplied to the test vessel at a constant flow rate of 85.8 Nm^3/min immediately after the start of Na leak.

(2) Terminating Na supply and oxygen gas supply

When one of the terminating conditions below is satisfied, the supply of both Na and oxygen gas is stopped.

Terminating Conditions:

- The cumulative amount of Na leak exceeds 2.4 ton.
- The inner pressure of test vessel exceeds 1.6 $kg/cm^2 \cdot g$.
- The temperature at ceiling and wall in test vessel exceeds 400°C (design temperature).
- When an emergency stop becomes necessary as a result of an unexpected occurrence.

(3) Storing Na drainage in Na catch pan

Na in the Na catch pan is drained to the impurities settling basin when the temperature of Na stored in the Na catch pan drops below 450°C and two hours have passed after the start of the Na leak. Records of the test progress are shown in Table 2.

4. RESULTS

4.1 Thermal Behavior of Test Pipe

Shown in Fig. 4.1 is the change with time in the temperature of outer surfaces of outer jacket of test pipe. Since the temperature changes at four thermocouples (TE1097, TE1096, TE1098, and TE1100) installed at the bottom of the outer surface of the outer jacket are similar to each other, the leaked Na spreaded uniformly along the bottom of the inner side of outer jacket in the direction of the length of piping.

Temperature (TE1099) at the top of piping clamp did not reach 500°C as Na leak temperature during the leak period. Thus the Na way not entered this place or entered only intermittently.

Temperature at thermocouples TE1097, TE1096, and TE1098 installed between the Na leak hole and clamp increased to 580°C maximum due to heat from Na combustion after the leak stopped. No temperature rise was seen at TE1100 installed outside the clamp after the leak was stopped. This occurred because Na leaking from the joints at the ends of the outer jacket accumulated in the insulating material covering at both ends of the specimen.

After the leak started a temperature peak appeared on the outer surfaces of all outer jackets. The video cameras showed that the combustion of inflammable gas occurred immediately after the leak started. The temperature peaks thus seem to be caused by the flame of this inflammable gas.

Figure 4.2 shows section A-A of the piping test specimen shown in Fig. 4.1. The temperature change at each portion of the section through the leak hole is shown. Temperature at the inner jacket (TE1089 and TE1091) was almost the same during the start of leak, that is, the temperature of leaked Na. After the leak stopped, the temperature dropped slowly. From these, it can be presumed that the runoff of Na from the leak hole spread across the annular space between inner jacket and piping without combustion therein.

An obvious temperature difference is recognized between the upper portion (TE1092) and lower portion (TE1093) of the insulating material. The temperature at the lower portion reached that true of leaked Na immediately after the leak started then remained almost constant during leak period. The temperature at the upper portion (TE1092), however, continued to rise even during the leak period. This occurred probably because Na flowed out from the joint and the opening for heater of inner jacket accumulated in the lower portion of the outer jacket, then gradually increased the Na level in the outer jacket.

The temperature at the lower portion of the outer jacket (TE1096) was almost the same as that of leaked Na and remained constant during Na leak period, but it fluctuated with time at the side and higher portions. At the upper portion (TE1094), the temperature reached 700°C in the last stage of leak. The latter high temperature can be explained by the combustion of inflammable gas at the outer surface of the outer jacket.

The above findings can be summarized as follows:

(1) The gap between the inner jacket and piping was filled up almost instantaneously by the Na flowing from the leak hole. Thereafter, Na flowed from the gaps in the inner jacket (joint and opening for heater in inner jacket) into the insulating material.

(2) Na flowing into the insulating material began to accumulate in the lower portion of the outer jacket. The accumulated Na then flowed out through the gaps in outer jacket, while causing the liquid level rise. The level increased further to the upper portion of piping by capillary action.

(3) There was no apparent temperature rise due to the reaction between Na and insulating material itself.

(4) When Na began to flow out from the joints in the outer jacket, an inflammable gas* was released causing burn**.

* This seems to be hydrogen generated from the reaction between Na and moisture contained in the insulating material.

** This was presumed from the results of photographing by video camera.

(5) The heat generated by the combustion of the inflammable gas and Na on the surface of outer jacket increased the temperature of the outer jacket and insulating material higher than the temperature of leaked Na soon after the Na leak began. However, they were cooled by the continuously leaking Na so that the temperature became almost the same as that of leaked Na (500°C) during the Na leak. However, the side and top of the simulated piping were not exposed to leaking Na, so the temperature fluctuated because of combustion heat and exceeded the temperature of leaking Na at some points even during the Na leak.

(6) When the Na leak stopped, the temperature of the outer jacket at the lower portion of piping, which had been cooled by the leaked Na, began to rise due to combustion heat of Na on the surface of the outer jacket then dropped upon completion of Na combustion.

4.2 Flow of Na and the Form of Leak

Figure 4.3 shows the change in pressure of cover gas of the Na heater and change in Na flow. The cover gas pressure during Na leakage was 3.7 $kg/cm^2 \cdot g$, almost the same as the 3.8 $kg/cm^2 \cdot g$ preset as test conditions, and remained constant.

The measured Na flow was 220 liters/min. (3.1 kg/s) and remained almost constant during the leakage. This almost agreed with 3.6 kg/s determined from the calculations in advance. The pressure loss coefficient of the test pipe seen from the leak hole in the simulated piping is calculated based on measured data as indicated below.

$$\eta = \frac{2 \cdot \Delta P \cdot A^2 \cdot \rho}{W^2} \qquad \text{(C)}$$

$$= \frac{2 \cdot 3.7 \cdot 9.804 \times 10^4 \cdot (2.3 \times 10^{-4})^2 \cdot 832}{3.1^2} = 3.33$$

Note*: Pressure loss and the level difference of Na in the middle of Na piping were very small and ignored here.

The form of leak of Na was checked by regularly arranging 137 thermocouples. Outputs from the thermocouples were processed by the graphic processing program "GRAPHMAN," and the results of temperature distribution in the space where Na leaked were expressed by constant temperature lines having the width of 100°C as shown in Fig. 4.4. This figure indicates the change in temperature distribution in the space below the simulated piping. The time elapsed from the start of test (opening of Na supply valve) is shown in the upper right corner. Na is supplied from the left side in this figure. As can be seen in this figure, Na began to leak from the piping approximately 7 seconds after the sodium valve opening. Figure 4.5 shows the gas temperature distribution at heights of 0.25 m, 1.0 m, and 1.5 m in the lateral section of the test vessel 10 seconds after the start of the test. From this figure, we can presumed that Na leaks out in a symmetrical pattern in the direction normal to the length of piping as shown in the sketch below.

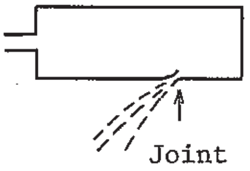

In the above sketch shown at the left, a falling Na has a velocity component in the direction of the length of piping (that is, not falling straight down) probably because Na leaked from the joint in the outer jacket. A temperature peak occurred even in the gas space below the simulated piping several seconds after the start of leak. Thereafter, however, the temperature peak occurred in the space near the falling point of Na on the floor, and the temperature peak in the intermediate space disappeared. Gas temperature was determined to reach 900°C several seconds after the leak started, because the temperature of combustion zone around a falling Na was measured. Figure 4.6 shows the temperature distribution every 10 seconds until one minute after the test start. The high temperature area in the gas space at first expanded as time elapsed, but this expansion stopped after 30 seconds and a quasi-false spray zone, as modeled in the analysis code, was formed.

Figure 4.7 shows a more detailed temperature distribution one minute after the test start. It clearly shows the presence of the quasi-false spray zone postulated in analysis codes. One minute after the test start, small high-temperature zones are recognized even in the space outside the spray zone.

In appendix, the temperature zone from the side and front of the simulated piping 2 ∿ 4 minutes after test start is shown.

The boundary of the quasi-false spray zone seen in Fig. 4.7 became less clear as time elapsed because the temperature became more uniform due to gas convection.

The Na leak continued about 13 minutes. Figure A-2 shows the cases even after the end of that leak. Though the zones with a temperature exceeding 700°C always existed before that, the maximum temperature was 600°C in the figure showing the case of 15 minutes later.

4.3 Change in Oxygen Concentration

The change in oxygen concentration with time is shown in Fig. 4.8. The maximum oxygen consumption rate determined from the change in oxygen concentration stated here is approximately 300 m^3/hr at the upper portion of SOLFA-2 test vessel, 210 m^3/hr at the middle portion, and 130 m^3/hr at the lower portion, and the average is 210 m^3/hr. (In this test, oxygen was supplied at the rate of 85.8 Nm^3/hr from the middle of test, but oxygen supply had not been started when the maximum value occurred.)

These values are oxygen gas consumption rate converted under normal temperature and pressure. By assuming 100% Na_2O_2 reaction, the average oxygen gas consumption rate can be converted into Na burning rate as shown below.

$$\frac{210 \times 2 \times 23}{22.4 \times 10^{-3} \times 3600} = 120 \text{ gNa/sec} \qquad \text{(D)}$$

$$2Na + O_2 \longrightarrow Na_2O_2$$

The above value is about 3.9% of the leaked Na since the flow of leaked Na was measured as 3,100 g/s in Section 4.2.

When one assumes 100% spray combustion as in the case of safety analysis in the actual plant, the proportion of burned Na to the flow of leaked Na becomes approximately 30%1). But, the present results clearly show that in a realistic leak from piping, the proportion is only one-tenth of that in the 100% spray combustion.

In the present case, the falling height of Na is almost half of that in the spray experiment. The one-tenth becomes one-fifth if Na burning rate is assumed to be almost proportional to its falling height. In any case, it has been substantiated that Monju's design concept ("Na leak from piping is assumed to be 100% spray") is sufficiently conservative with respect to the Na burning rate.

4.4 Changes in Gas Pressure and Temperature

Figure 4.9 shows how gas pressure in the SOLFA-2 vessel changed with time, and Fig. 4.10 shows the gas temperature at three points with different height in the upper portion of the simulated piping.

Although the space in the upper portion of the simulated piping has a large volume (about 6 m from piping to the top of vessel), it exhibits almost no gas temperature difference between these points because of a vigorous convection.

The gas temperature suddenly rises after the Na leak starts, drops after reaching the maximum of 450°C, becomes almost constant near the end of Na leak, then suddenly drops after the Na leak stops. Gas pressure shows a similar tendency; its maximum pressure reaches 0.9 $kg/cm^2 \cdot g$. However, in the present test, oxygen gas was supplied in the middle of test, 2.4 minutes after start of Na leak. Because of this oxygen gas supply, the pressure increased near the end of Na leak when combustion calmed down. The relation between the change in gas pressure and change in the mean gas temperature with time will now be compared. The volume of the space above the catch pan is 95.5 m^3. Assuming adiabatic expansion of gas, the maximum gas pressure can be calculated as shown below from the law of ideal gas.

$$\frac{P_f}{P_i} = \frac{T_f + 273.15}{T_i + 273.15} \qquad (E)$$

$$= 2.34\ \mathrm{kg/cm^2 \cdot a}$$
$$= 1.34\ \mathrm{kg/cm^2 \cdot g}$$

where,

P_i: Initial gas pressure (1.014 kg/cm^2·g)
T_i: Initial gas temperature (40°C)
T_f: Gas temperature when reaching maximum pressure (450°C)

The above is considerably larger than the measured value of 0.9 kg/cm^2·g. This probably caused by the following two reasons:

(1) Decrease in oxygen due to combustion.
(2) Pressure relief to the gas space below the catch pan (a gas leak is present through the catch pan mounting portion in the zone between the upper and lower spaces).

To clarify the above, the following correction were made to the measured pressure of 1.34 kg/cm^2·g by taking into account of the two factors stated above:

Let the gas is an ideal gas, the initial state of test is expressed by i, and the state of reaching maximum pressure is f, then the following equations are derived:

$$P_i\ (V_1 + V_2) = (n_{N2} + n^i{}_{O2})\ RT_i \qquad \text{(F)}$$
$$P_f\ V_1 = (n^f{}_{N2,1} + n^f{}_{O2,1})\ RT_1$$
$$P_f\ V_2 = (n^f{}_{N2,2} + n^f{}_{O2,2})\ RT_2$$

where,

V_1, $n_{O2,1}$, $n_{N2,1}$: Volume above catch pan, and mol number of O_2 and N_2
V_2, $n_{O2,2}$, $n_{N2,2}$: Volume below catch pan, and mol number of O_2 and N_2

From the measured results, the oxygen consumption rate is about 21%/7 minutes as average of upper and lower portions, and the time of reaching maximum gas pressure is about 2 minutes. Thus, no is equivalent to 15 mol%.

From the above equation, the following equation is derived:

$$n^f{}_{N2,1} + n^f{}_{O_2,1} + n^f{}_{N2,2} + n^f{}_{O_2,2} = \frac{P_f}{R}\left(\frac{V_1}{T_2^f} + \frac{V_2}{T_2^f}\right) = n_{N2} + n^f{}_{O_2}$$
$$= \frac{P_i}{RT_i}(V_1 + V_2)\cdot(1.-(0.21-0.15))$$

therefore, (G)

$$\frac{V_1}{T_1^f} + \frac{V_2}{T_2^f} = \frac{P_i}{P_f}\quad\frac{V_1 + V_2}{T_i}\cdot 0.94 \qquad \text{(H)}$$

In this case, $V_1 = 95.5\ m^3$, $V_2 = 15.5\ m^3$, $T_2 = 70°C*$, and $T_1 = 450PC$, therefore,

$$P_f = P_i\cdot\frac{V_1 + V_2}{T_i}\cdot 0.94 \,/\, \left(\frac{V_1}{T_1^f} + \frac{V_2}{T_2^f}\right) = 1.88\ kg/cm^2\cdot a \qquad \text{(I)}$$
$$= 0.88\ kg/cm^2\cdot g$$

Note*: Measured value for the space below catch pan about 2 minutes later (mean temperature of TE2090, 2091, and 2092).

The above value agrees fairly well with the measured value. Thus, we can see that the gas pressure will correspond to gas temperature if we properly evaluate the gas leak to gas space below catch pan through the catch pan mounting.

4.5 Temperature of Na Pool on Catch Pan and of Structures

Figure 4.11 shows the change in temperature of a Na accumulated in the catch pan at two places: bottom of the pan and 10 cm above the bottom. Ten centimeters above the bottom, the temperature reached the peak of 960°C in the first several minutes due to the flame of falling Na. Since the flow of Na leak is 3.1 kg/s and the diameter of the catch pan is 3.4 m, the rate of Na liquid level increase in the catch pan can be given by the following equation based on the burning rate of 4% in the space where Na falls:

Eq. J:

$$\frac{(1-0.04) \times 3.1/832}{3.4^2 \times \frac{\pi}{4}} \times 100 \times 60 = 2.4 \text{ (cm/min.)}. \qquad \text{(J)}$$

The above means that the depth becomes 10 cm in about 4 minutes. Also in Fig. 4.11, the temperature becomes 600°C about 4 minutes later, which is the essential temperature of Na pool.

This occurs because Na is heated by a burning while it falls. After the Na leak ends, the temperature of the Na pool drops simply because of the oxygen supply terminates.

Figure 4.12 shows the duration of temperature change at various parts of the test vessel. This shows the outer surface temperature of the top end plate of test vessel (A), the inner surface temperature of the top end plate (B), the inner surface temperature of the side wall (C), and gas temperature inside the jacket (D) (no water was placed in water-cooling jacket in the present experiment). In this figure, the temperature at the top is higher than that at the side, probably because a hot gas rose due to gas convection, thereby applying more heat to the top than to the side.

Figure 4.13 shows the heat flux transferred to the wall as obtained by the two heat flux meters mounted inside the side wall of the test vessel and its change with time. The results of the Na leak test RUN-B3[2)] with a simulated piping (conducted previously) indicated that the surface temperature of the outer jacket became quite high (750°C) because of a Na combustion on the surface of the outer jacket, and the analysis conducted after RUN-B3 by ASSCOPS code pointed out the importance of thermal radiation from the surface of the outer jacket. Therefore, two heat flux meters were installed on the wall. The difference between the outputs from the exposed heat flux meter and the shielded heat flux meter corresponds to the heat flux due to radiation from the surface of piping.

The results indicated that a difference of the heat flux from the two meters is considerably smaller. It can be concluded, therefore, that the radiation energy becomes small as the combustion progresses and a large amount of aerosol contained in it.

4.6 Energy Balance

Na leaking from the simulated piping burns and heats up itself during a fall then is accumulated and burns in the catch pan, thereby transferring heat to the catch pan and surrounding structural materials. Gas heated to a high temperature transfers the heat to the test vessel. Thus, the energy generated by the combustion finally balances with the temperature increment at each part of the test vessel. The temperature at each part of the test vessel was measured by thermocouples. Therefore, combustion energy can be derived from these data. In evaluating the energy balance, only those structural members for which the size of heat capacity and degree of temperature rise could not be neglected were selected. Figure 4.14 indicates the measuring positions considered in evaluating the energy balance and the numbers of thermocouples used for measuring typical temperatures at the measuring positions.

The test vessel showed no uniform temperature rise as a whole. Instead, the slope width of the temperature rise at each part was not the same. Thus, in the evaluation the vessel was divided into seven portions: top portion of vessel (WALL1) where the temperature is rather uniform, upper portion of vessel (WALL2), lower portion of drum (WALL3), bottom of catch pan (FLOOR1), catch pan-supporting flange (FLOOR2), side portion of catch pan (FLOOR3), and bottom of vessel (FLOOR4). Temperature at each portion was averaged with respect to inner and outer surfaces, and the average of the mean temperature of inner surface and the mean temperature of outer surface obtained was used as the representative temperature.

The gas was evaluated for the upper and lower portions. However, it heat capacity is small as stated later, thus, its contribution to the overall energy balance was neglected.

Energy balance at time t can be expressed by the following equation:

$$q_{heat} = WC_p\ (T_{POOL} - T_{IN}) + M_{gas}\ C_p\ \dot{T}_{gas} + M_{wall}\ C_p\ T_{wall} \qquad \text{(K)}$$
$$+ M_{FLOOr}\ P_p\ \dot{T}_{FLOOr}$$

where,

q_{heat}: Heat generated by combustion (kcal/sec.)
W : Flow of leaked Na (kg/sec.)
C_p : Specific heat (kcal/kg°C)
M : Weight (kg)
T, $\dot{T}$: Temperature (°C) and rate of temperature change (°C/sec.)

From the above equation, the change in generated heat with time can be evaluated. Each term of the above equation was calculated using data obtained 10 minutes from the start of leak. Figure 4.16 shows the changes in the energy of gas and the latent heat of Na (first term of the right expression of the above equation), Fig. 4.17 the change in energy at the wall on the vessel side, and Fig. 4.18 the change in energy at the catch pan and at the bottom of the vessel.

From Fig. 4.16, we can see that the change in energy possessed by gas is one order of magnitude smaller than other terms. From Fig. 4.15, combustion heat was stable at 3,000 kcal/sec for the first 90 seconds then 300 to 400 kcal/sec thereafter during the leak period. To convert from combustion heat to Na consumption rate, the reaction heat was expressed by the following equation assuming the formation reaction of 100%Na_2O_2:

$$2Na(l) + O_2(g) \longrightarrow Na_2O_2(s) \qquad \text{(L)}$$
$$\Delta H = 2696\ \text{kcal/kgNa}$$

The Na consumption rate can be obtained by dividing the combustion heat of the above by ΔH. Also, since the change in oxygen concentration with time was obtained in Section 4.3, it is possible to obtain the consumption rate of Na independently from the evaluation made here. Values obtained from both the methods are shown in Fig. 4.19. To find the Na consumption from the change in oxygen concentration with time, the following equation was used:

$$-\dot{m}_{Na} = \frac{23}{16}\,\frac{\dot{m}^{i}{}_{02}}{C^{i}{}_{02}} \cdot \dot{C}_{02} = \frac{23}{16}\,\frac{\dfrac{1.013\times10^{5}\cdot95.5}{8.3168\cdot300}\cdot 0.21 \cdot 32\times10^{-3}}{0.21}\cdot \dot{C}_{02} \qquad \text{(M)}$$

$$= \frac{23}{16} \cdot 124\ \dot{C}_{02} = 178 \cdot \dot{C}_{02}$$

where,

$\dot{m}_{Na}$, $\dot{m}_{02}$: Consumption of Na and O_2 by combustion (kg/s)

$\dot{C}_{02}$: Change in oxygen concentration (-/sec.)

Since the above equation does not contain the portion of filled oxygen*, overall consumption can be obtained from the following:

$$\dot{m}_{Na} = -178 \cdot \dot{C}_{02} + \frac{1.013 \cdot 10^{5} \cdot 85.5}{8.3169 \cdot 300} \cdot 32 \cdot 10^{-3} \cdot \frac{23}{16} \;/\; 3600 \qquad \text{(N)}$$

$$= -178 \cdot \dot{C}_{02} + 0.044 \ \text{(kg/s)}$$

Note *: Oxygen was supplied 144 seconds after the start of leak.

The following can be learned from Fig. 4.19: At first, the burning rate of Na obtained from energy balance for 100 seconds after the start of combustion was extremely large, but, thereafter, reached a relatively stable value of 150 g/sec. This agrees fairly well with the solid line (value obtained from the measured value of oxygen gas) shown in the figure. From the above, the burning rate of Na leaking from the simulated piping is between 100 and 200 g•Na/sec.

The Na burning rate obtained from the energy balance for 100 seconds in an early stage was very large because the average value for inner and outer surfaces was adopted as the representative temperature in calculating energy absorbed by structural members (i.e., the thermocouples installed for measuring the surface temperature inside the structural members were exposed to high-temperature gases). Thus, the thermocouples sensed gas temperature near the wall is easily understandable from Fig. 4.12 (A), so that temperatures higher than the actual surface temperature inside the vessel were indicated. Therefore, the absorption energy became higher than the actual one if that kind of temperature is adopted as representative temperature of the vessel. Results of reexamining absorption energy are shown by broken lines in Fig. 4.19. In this case, the disturbance due to the convection of high temperature gas in the early stage was considerably reduced.

4.7 Post-Test Examination of Simulated Sodium Pipe

After stabilizing the sodium chemically by carbon dioxide, we removed the test pipe from the vessel and examined it. Details were photographed by video cameras and 35 mm cameras. Findings of the visual observation are explained below.

(1) A large amount of Na aerosol deposited on the surfaces of the outer jacket, but there were no damage to the jacket itself and its joints.

(2) A large amount of metal Na was present in the insulating material covering both ends of the pipe. This probably occurred because the Na, which leaked from the joints at both ends of the outer jacket, flowed into the insulating material covering both the ends and remained as metal Na in the insulating material since there was no passage for leakage in the cover for insulating material at both the ends.

(3) Tested insulating material changed its color to black and became brittle, but its original shape was maintained without indicating any trace of a chemical reaction with Na.

(4) Metal Na in the insulating material remained around the whole perimeter of the leak hole and in the lower half in other portions.

(5) The inner jacket was sound, and the spacer and the opening for the simulated heater remained the same as before the test without deformation.

(6) The piping itself was sound, and the leak hole made in advance maintained its original shape.

5. CONCLUSIONS

The Na leak test (RUN-E2) from simulated Na piping was conducted using the SOLFA-2 test vessel in SAPFIRE facility. In this test, the SOLFA-2 vessel was closed and sealed, and the piping model with a reduced scale of 1/3.5 of the secondary system of Monju was placed inside the closed vessel. A leak hole with the reduced scale of 1/4 Dt leak hole area of the actual plant was made in the pipe, and Na was forced to leak by applying a pressure equal to the system pressure of 3.8 $kg/cm^2 \cdot g$ in the hot leg of the secondary system of the actual plant. Duration of leak was approximately 13 minutes.

Principal test results are as follows:

(1) Thermal behavior of test pipe

- Piping, outer jacket, and inner jacket were in good shape without corroded by Na and broken by high temperature.
- There was no obvious temperature rise due to reaction between Na and the insulating material.
- Na began to leak out mainly from the lower joint of the outer jacket; and an inflammable gas was immediately released and burnt.
- When the Na leak stopped, the temperature of the lower outer jacket, which was previously equal to the temperature of the flowing Na, rose until Na combustion on the surface was terminated.

(2) Na leak flow

- Na leak flow rate was 3.1 kg/sec as predicted before the test and remained almost constant during the leak.

(3) Others

- Na combustion rate was about 120 gNa/sec assuming of Na_2O_2 formation. This value is equivalent to about 4% of the flow of leaked Na.
- The maximum temperature of the gas below the test pipe was 900°C, the inner temperature of test vessel was 600°C, and the maximum temperature in the burning zone on the surface of the pool was about 950°C.

- Maximum temperatures of the test vessel above the test pipe were approximately 200°C at the inner surface of ceiling, 130°C at the outer surface of ceiling, and 80°C at the inner surface of sidewall and gas within jacket.
- Maximum temperatures and pressure of gas inside the test vessel were about 450°C and 0.8 $kg/cm^2 \cdot g$.

The above results substantiated that the insulation structure around the piping fully prevented the spray type leak of Na thereby protecting its integrity from Na leakage and combustion during the accident. In addition, the combustion rate of Na at that time was about 4% of the flow of leaked Na. This means that the combustion due to realistic leakage of Na from piping is very mild compared to spray type combustion, considering that the combustion rate of Na was about 30% of the flow of leaked Na in the complete spray type combustion test conducted previously.

REFERENCES

1) Morii, T. and Fukuchi, T. et al.: Large-Scale Sodium Leak and Combustion Test (III) ... Large-Scale Na Spray Combustion Test in Air Atmosphere, RUN-E1, PNC SN9410 86-124, December 1986.

2) Himeno, Y. and Miyahara, S.: Basic Tests on Sodium Fire Protection Facilities (III) ... Reduced-Scale Model Test on the Progress of Sodium Fire in Secondary Circuit, RUN-B3, PNC SN941 85-130, September 1985.

3) Hoshi and Nei: Rupture Test on Insulation Structure for Secondary Main Cooling Piping, PNC ZJ201 83-16, May 1983.

Table-1 Pressure Loss Coefficient of Simulated Sodium Pipes

	Fluid	Area of Leak Hole** (cm^2)	Fluid Pressure ($kg/cm^2 \cdot g$)	Flow Rate (kg/s)	Pressure Loss Coefficient*** (−)
Water Test by PNC* (Straight Pipe)	Water	15.0	5.8	29.9	2.85
〃	〃	〃	5.5	28.9	2.89
〃	〃	〃	3.8	25.0	2.69
〃	〃	〃	2.4	20.0	2.65
Water Test by Toshiba (Straight Pipe)	〃	〃	6.41	35.1	2.3
〃 (Elbow Pipe with Insulator)	〃	〃	6.68	33.9	2.56
RUN-B3	Na	10.0	0.25	0.832	58.9
Data for "Monju"	〃	15.0	6.0	33.0	1.0

* These Pipes are Actual Dimensions with no Insulator

** Area of the Leak Hole

*** Pressure Loss Coefficient is Defined as Following

$$P = \frac{1}{2} \eta \rho v^2$$

P : Fluid Pressure

η : Pressure Loss Coefficient

ρ : Fluid Density

V : Flow Velocity at the Leak Hole ($= W / \rho \cdot A$)

W : Flow Rate

A : Area of Leak Hole

(PSS-SFE-404)

Table-2 Progression of RUN-E2 Test

Time	Test Progression
11/12	
10 : 12	Sodium Charge in Sodium Heater
13 : 02	Start Heating up of Sodium Heater (250℃)
11/13	
11 : 32	Data Input of Stop Conditions to CENTUM
11 : 02	Start Aerosol Scrubber
	Completion of Heating of Sodium Heater (505℃)
14 : 20	Stop Cover Gas Control
14 : 20	Start Pressurizing Cover Gas of Sodium Heater
14 : 10	Switch Off SCR Control Heater
14 : 52	Start Data Recording
14 : 55	Start Sodium Feed to Simulated Sodium Pipe
15 : 00	Start Oxygen Gas Supply (85.8N/hr)
15 : 10	Stop Sodium Feed
15 : 10	Stop Oxygen Gas Supply
15 : 15	Gas Blow of Sodium Heater
15 : 33	Change Temperature Level of Pre-Heating of Sodium Piping (505℃ → 250℃)
16 : 40	Drain Remaining Sodium in Catch Pan
	Stop Aerosol Scrubber
	Holding the Conditions
15 : 15	Start Cover Gas Control of Test Vessel
	Stop Data Recording
	Drain of Remaining Sodium from Test Vessel

(PSS-SFE-386)

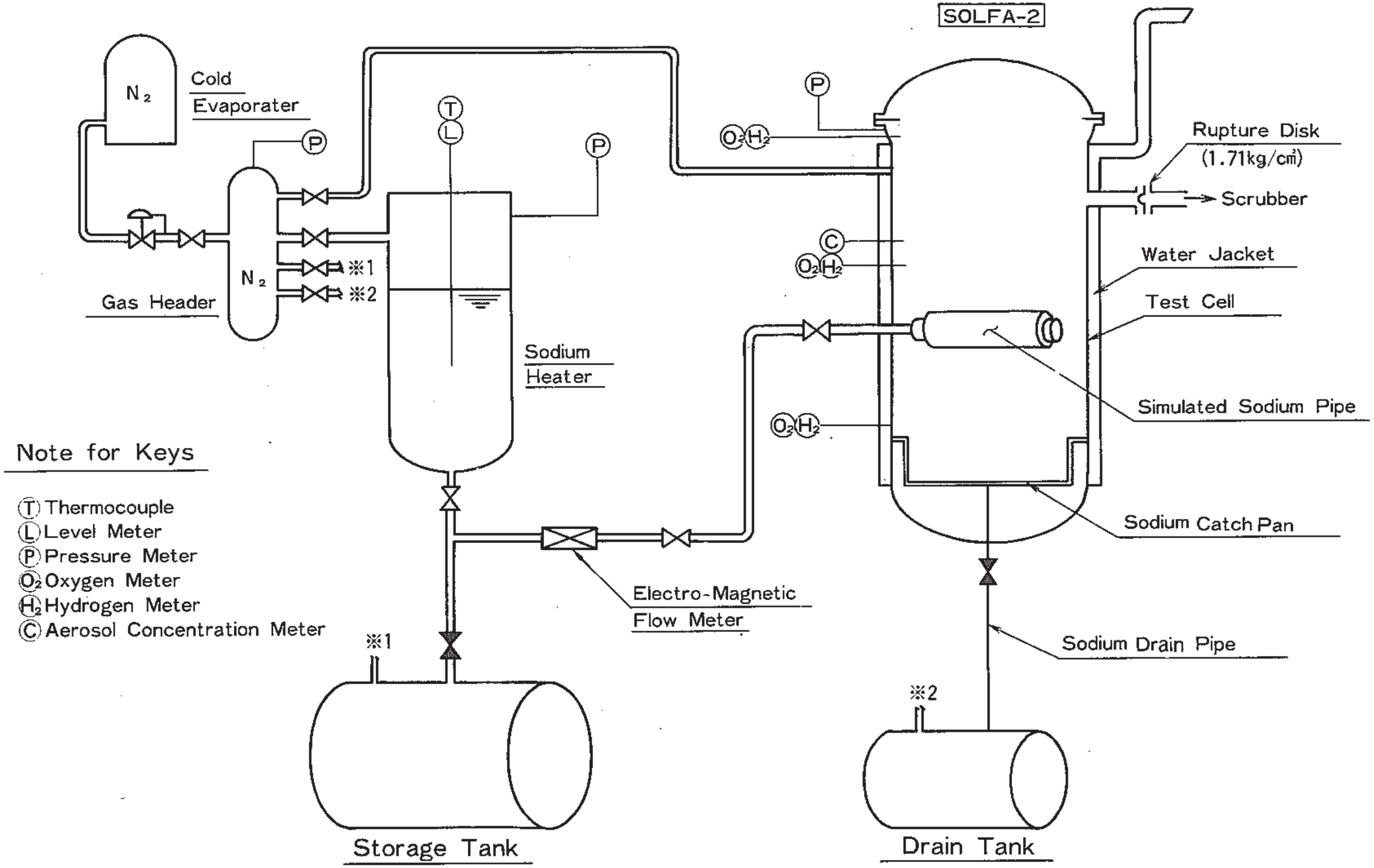

Fig. 2.1 Arrangement of Test Rig for Run-E2

(PSS - SFE - 387)

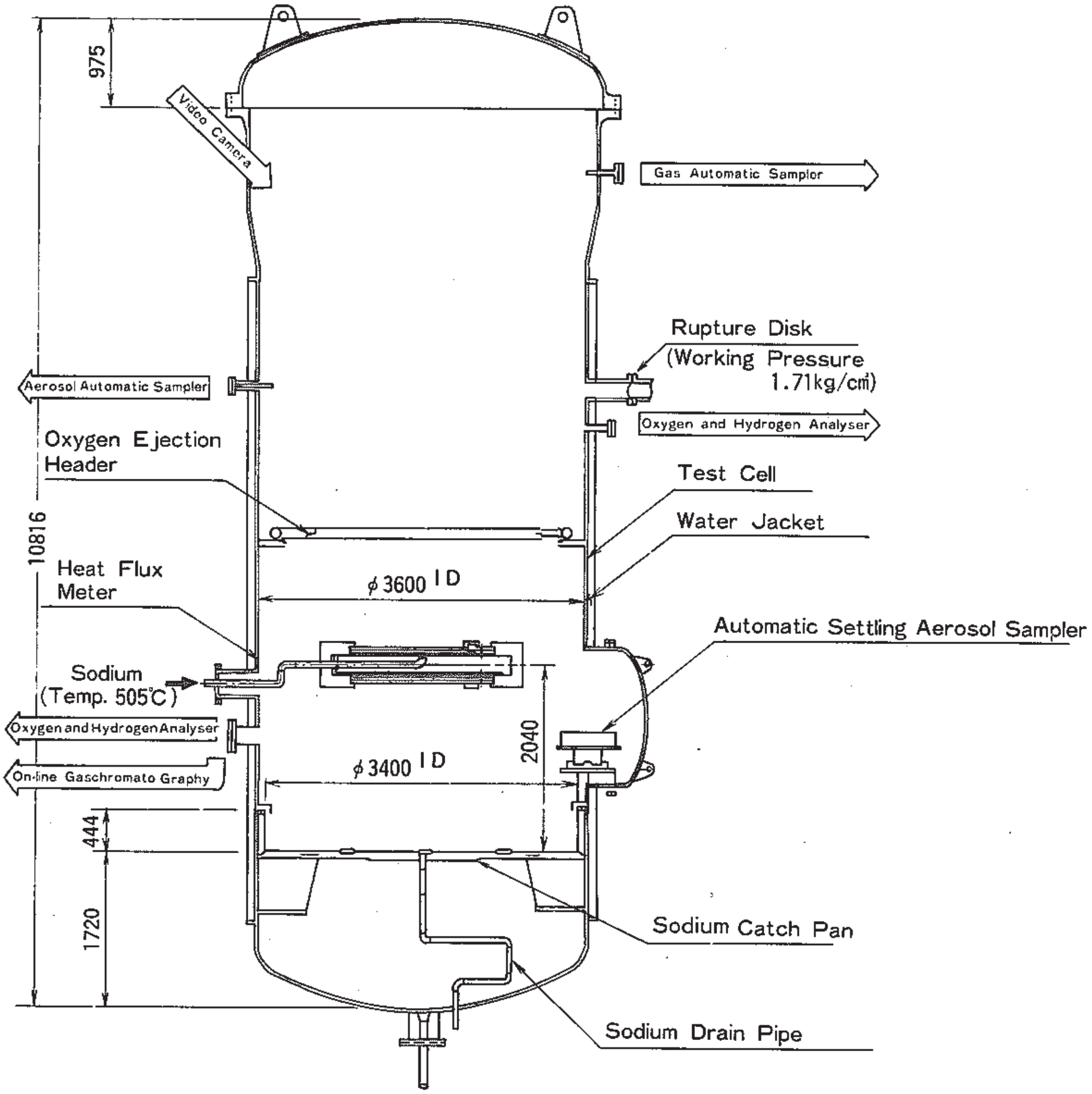

Fig. 2.2 SOLFA-2 Overview

(PSS - SFE - 388)

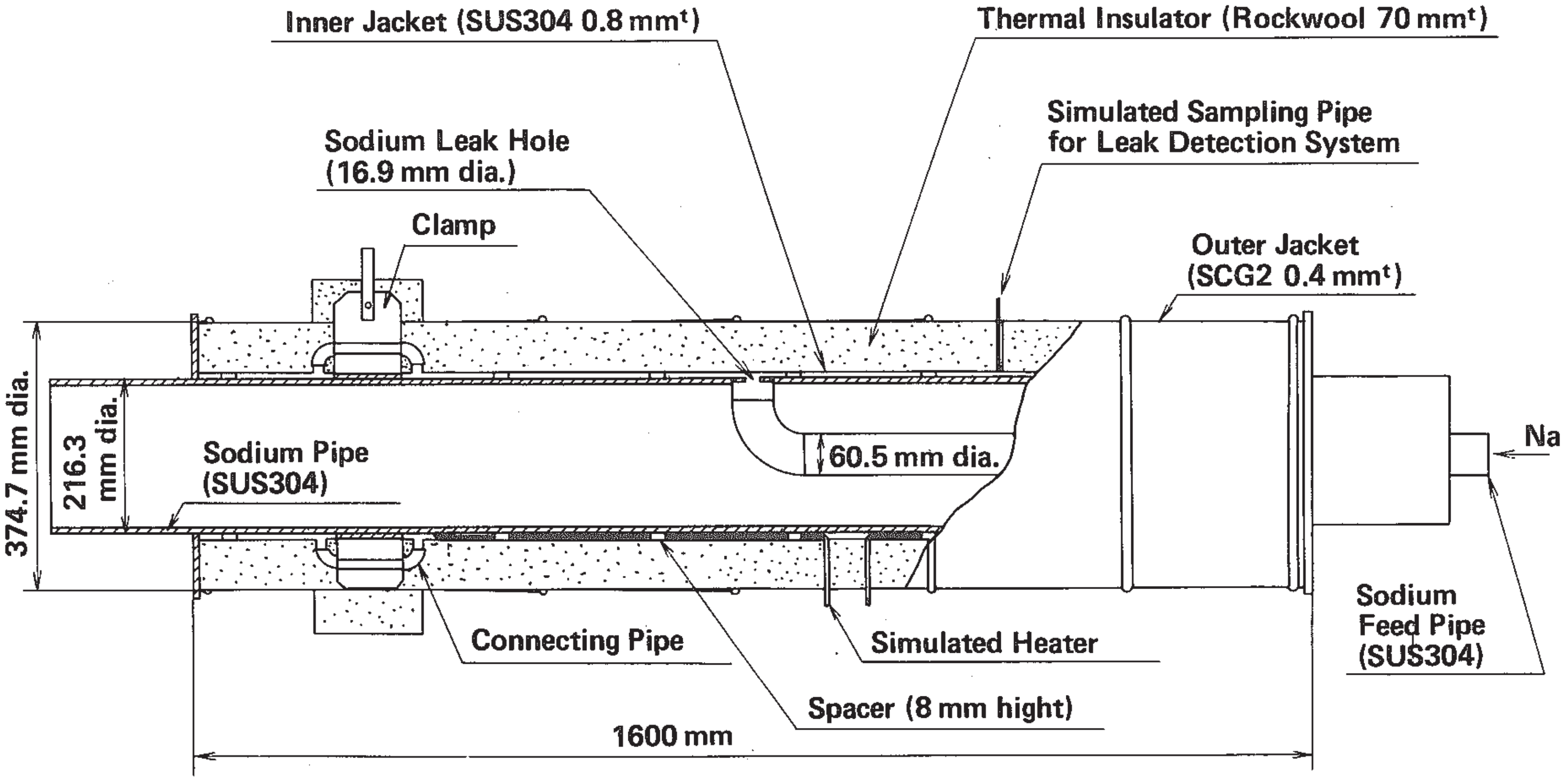

Fig.2.3 Cut View of Simulated Sodium Pipe for Run-E2

PSS-SFE-354

SOLFA-2 Cut View of Simulated Sodium Pipe

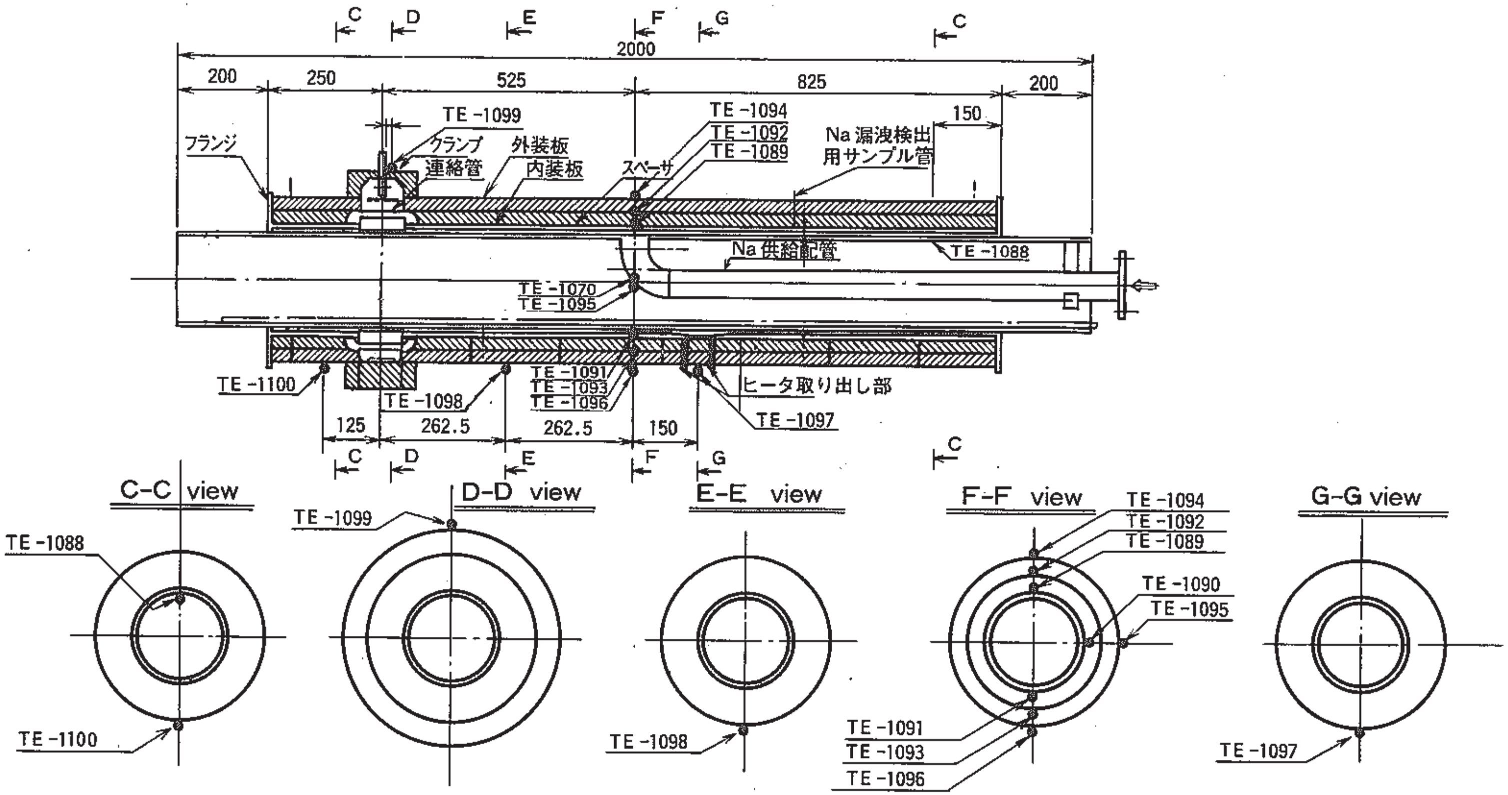

Fig. 2.4 Locations of the Thermocouples Attached to the Simulated Sodium Pipe

(PSS - SFE - 389)

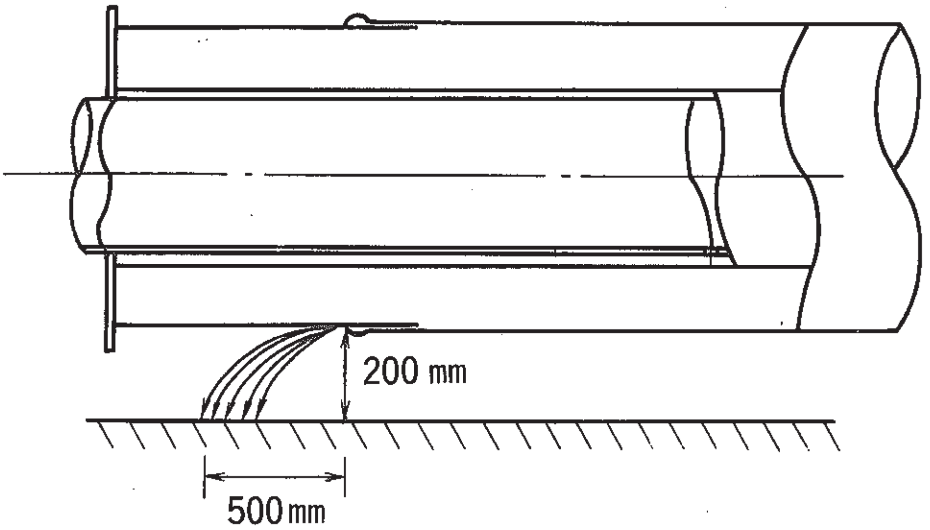

Fig. 2.5 Leakage Flow Pattern from Mock-up Straight Pipe

- Water Simulation Test -

(PSS - SFE - 390)

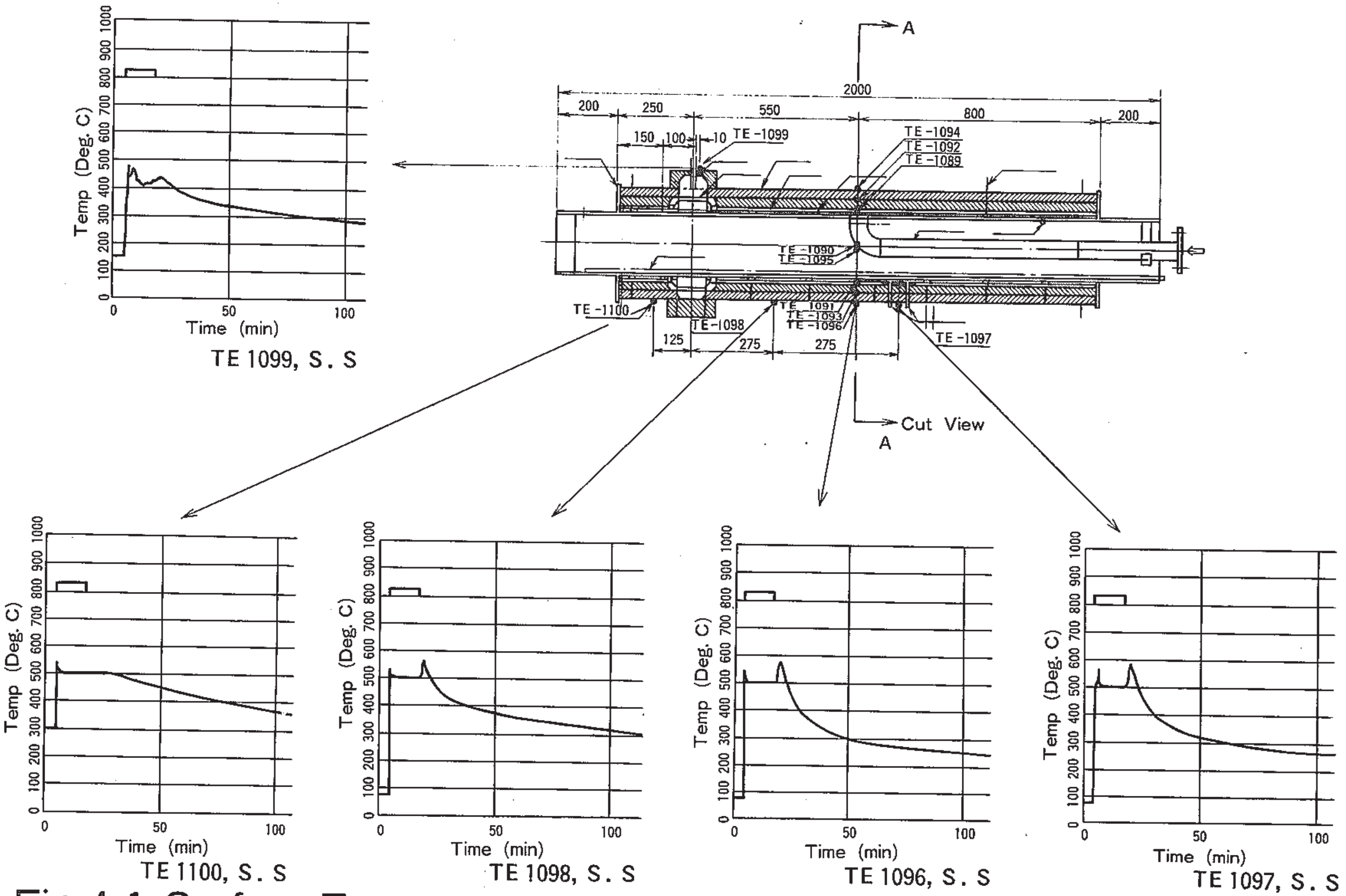

Fig. 4.1 Surface Temperatures of Outer Jacket of Simulated Sodium Pipe
(PSS - SFE - 391)

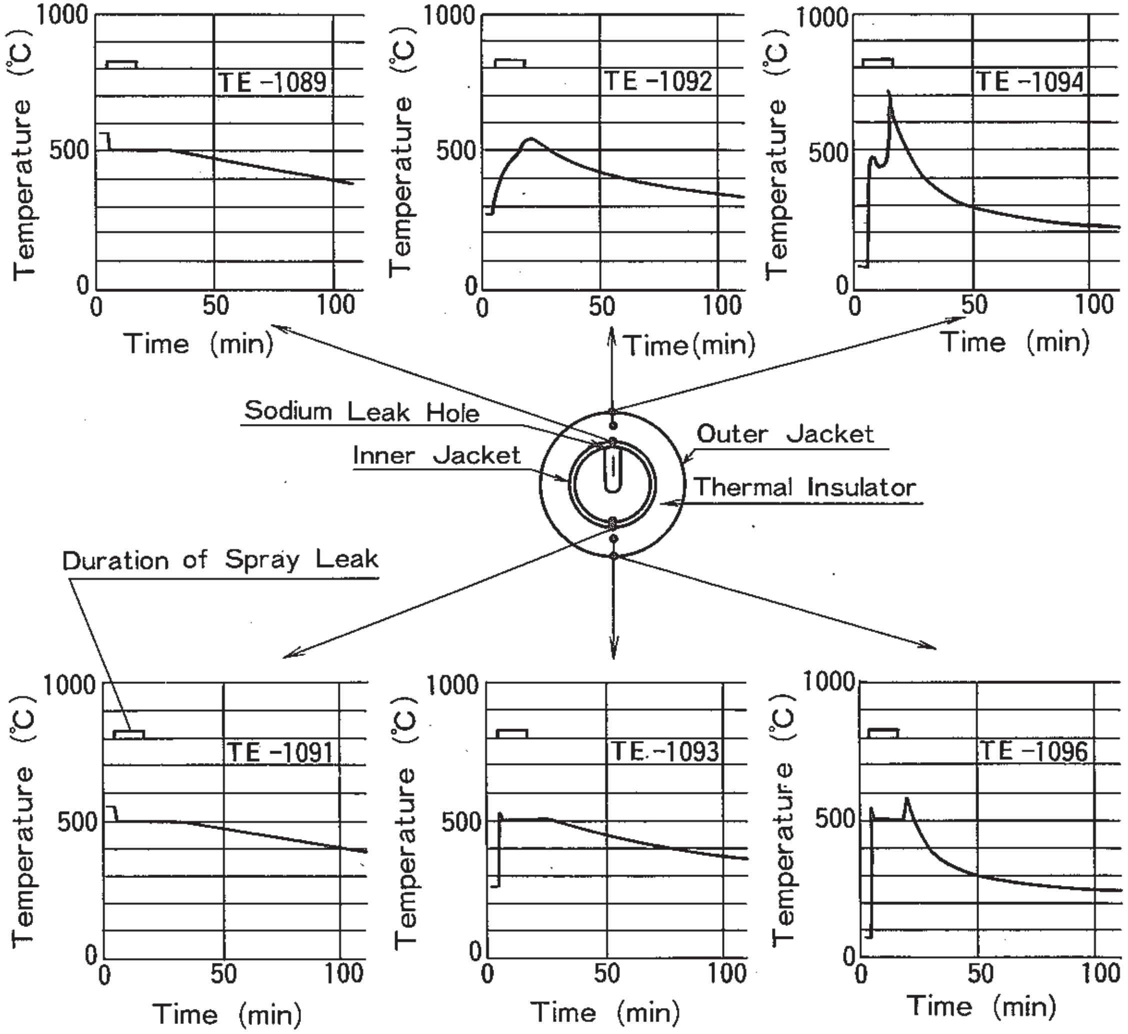

Fig. 4.2 Temperature Histories of Simulated Sodium Pipe

(PSS - SFE 392)

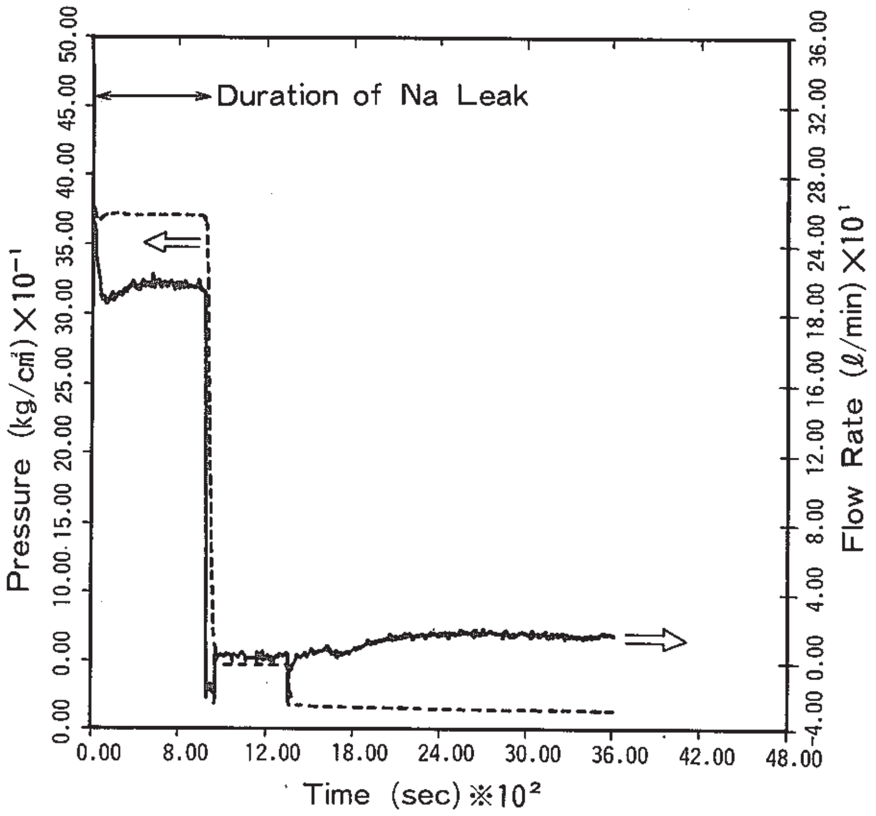

Fig. 4.3 Records of Cover Gas Pressure in Sodium Heater and Sodium Leak Rate

(PSS - SFE 393)

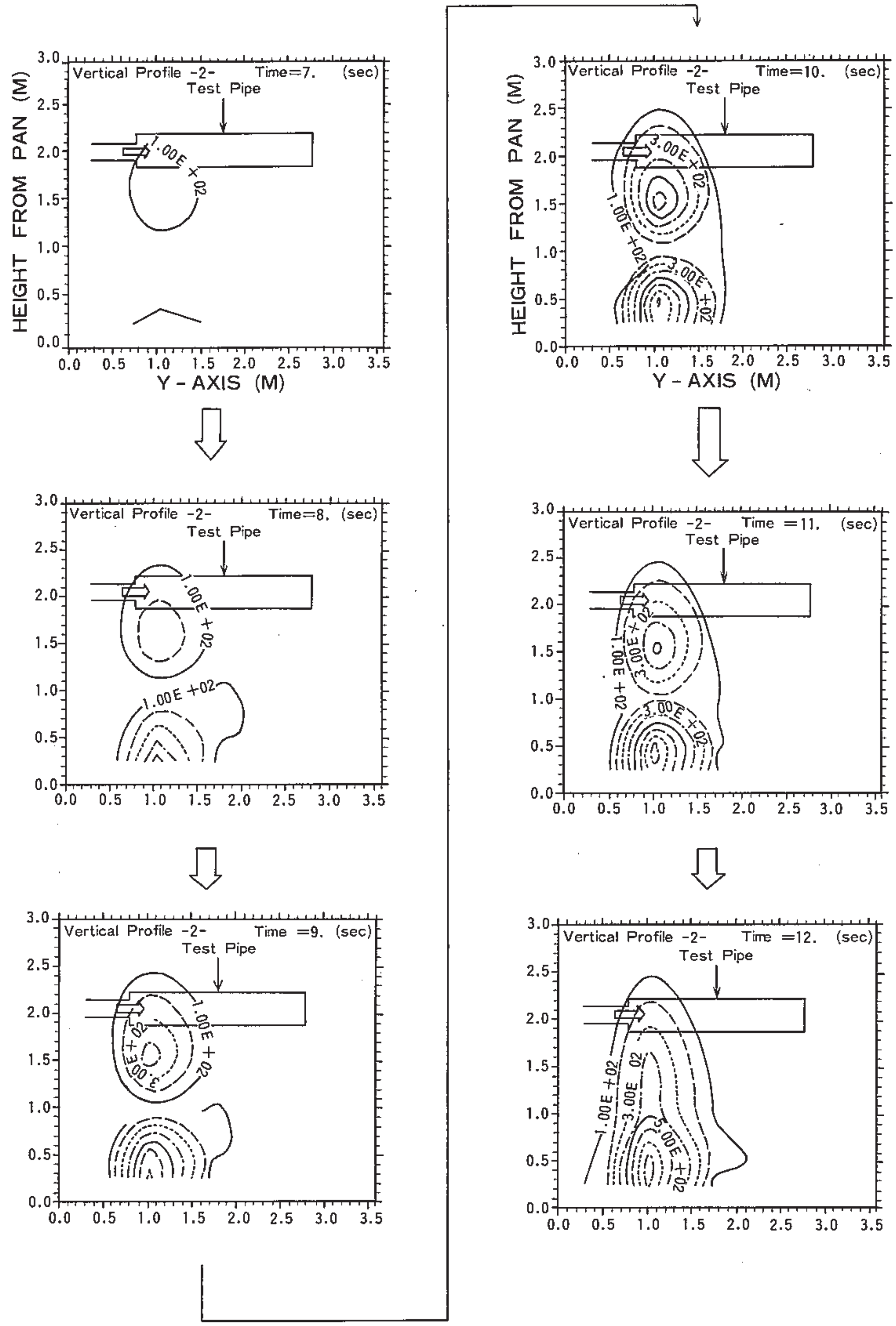

Fig. 4.4 Temperature Profiles in Gas Phase below Simulated Sodium Pipe (Vertical Profiles)
(PSS - SFE 394)

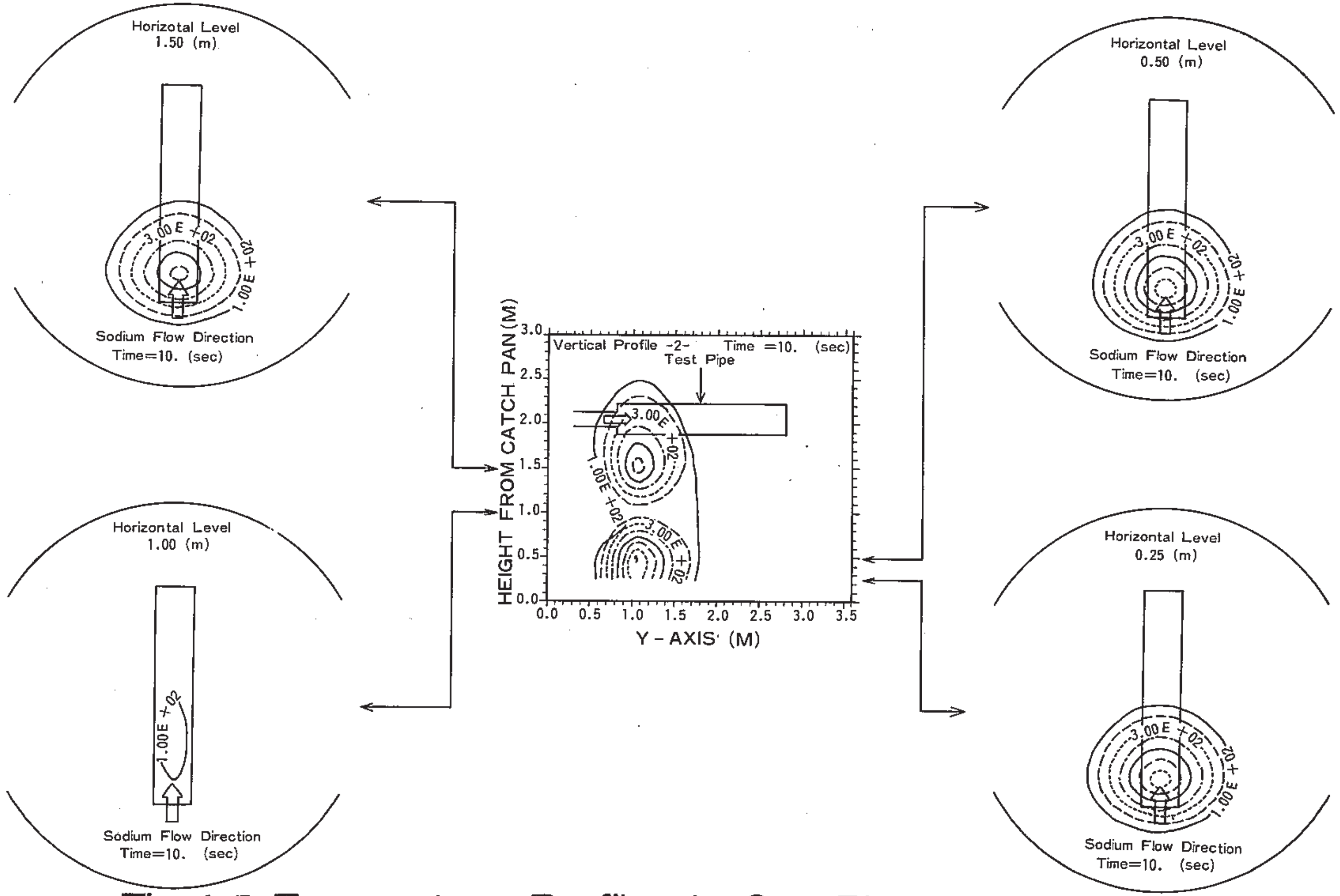

Fig. 4.5 Temperature Profiles in Gas Phase below Simulated Sodium Pipe (Horizontal Profiles) (PSS - SFE 395)

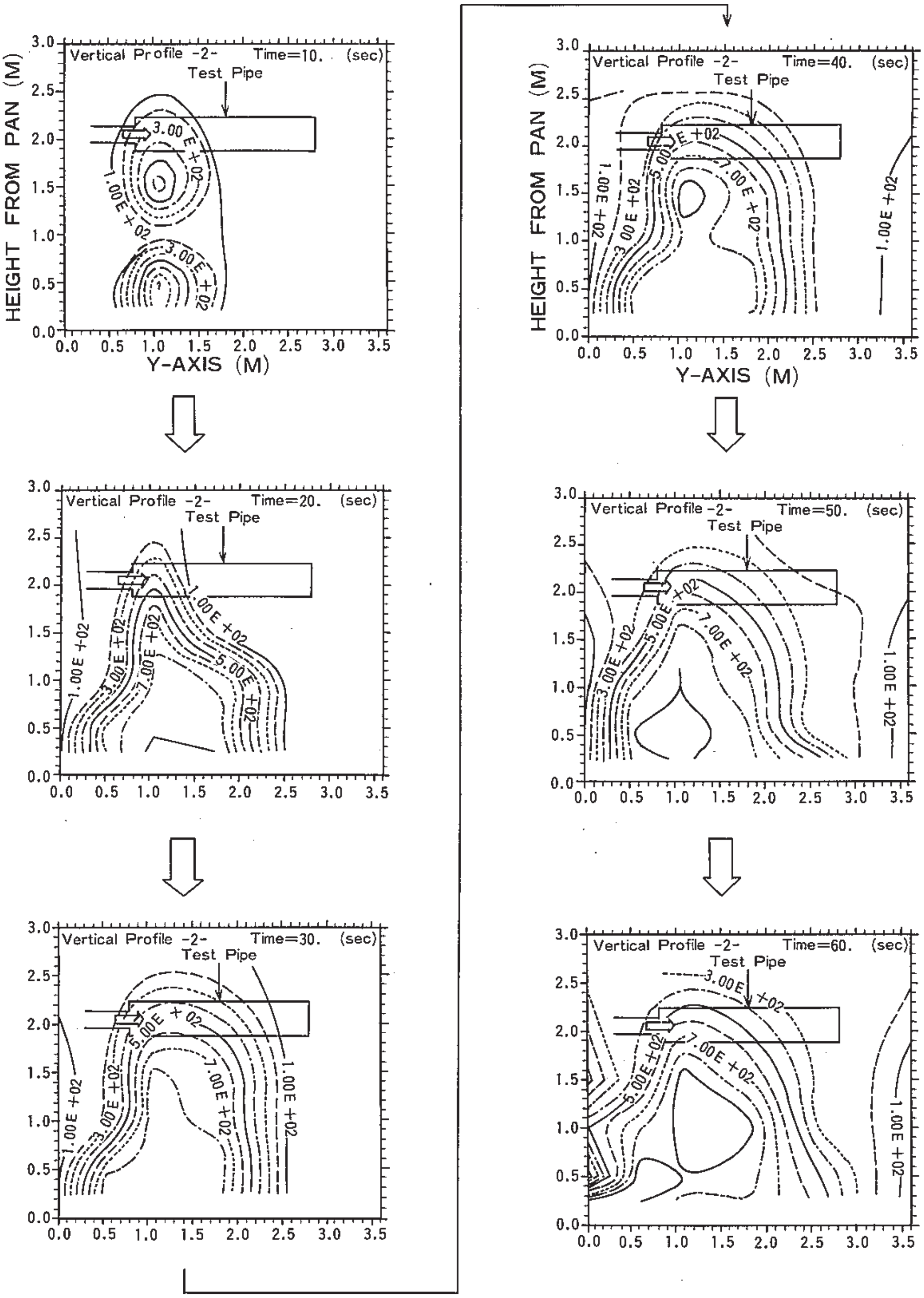

Fig. 4.6 Temperature Profiles in Gas Phase below Simulated Sodium (Vertical Profiles)

(PSS - SFE 396)

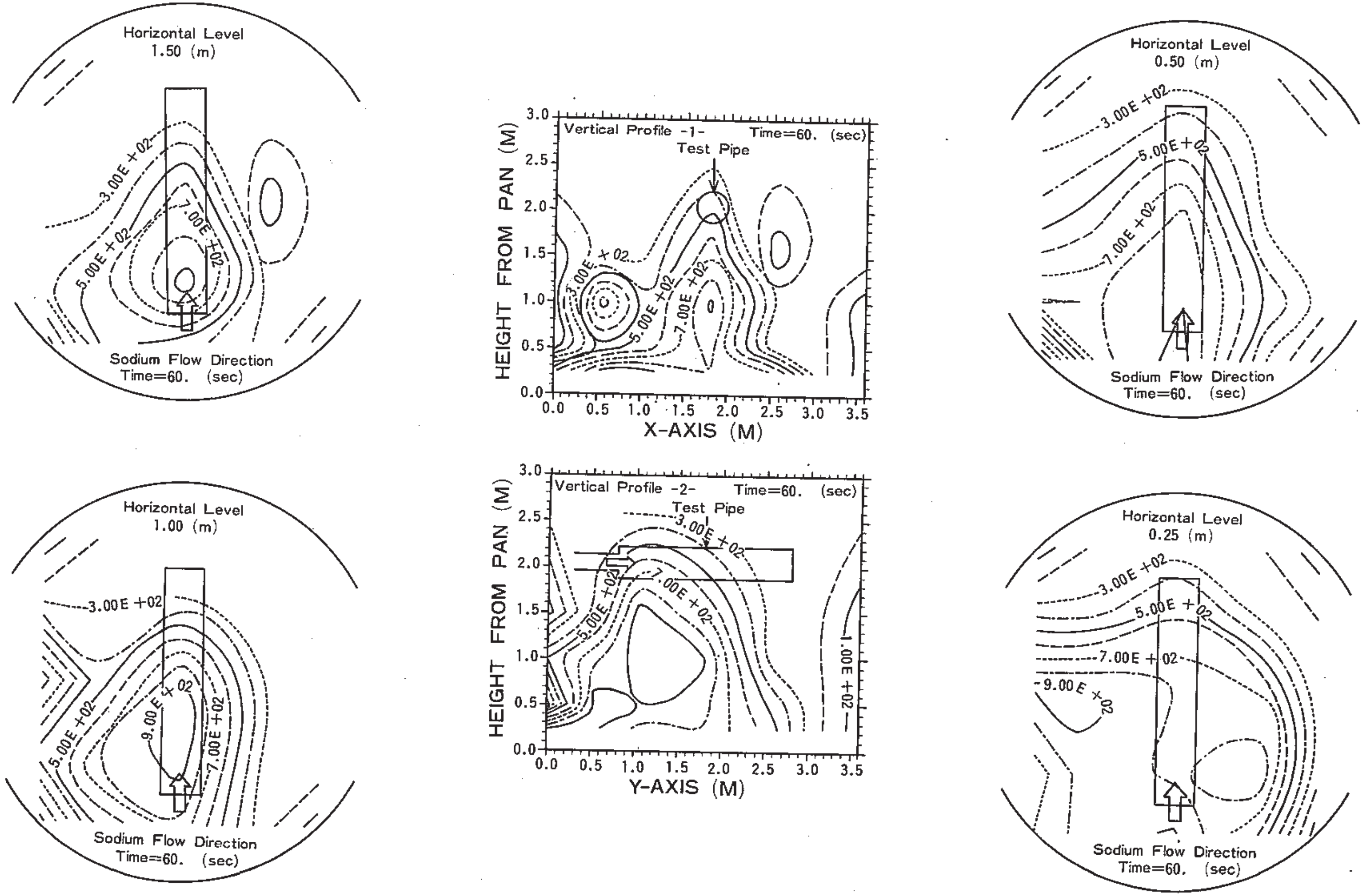

Fig. 4.7 Temperature Profiles in Gas Phase below Simulated Sodium Pipe (Horizantal Profiles)

(PSS - SFE - 397)

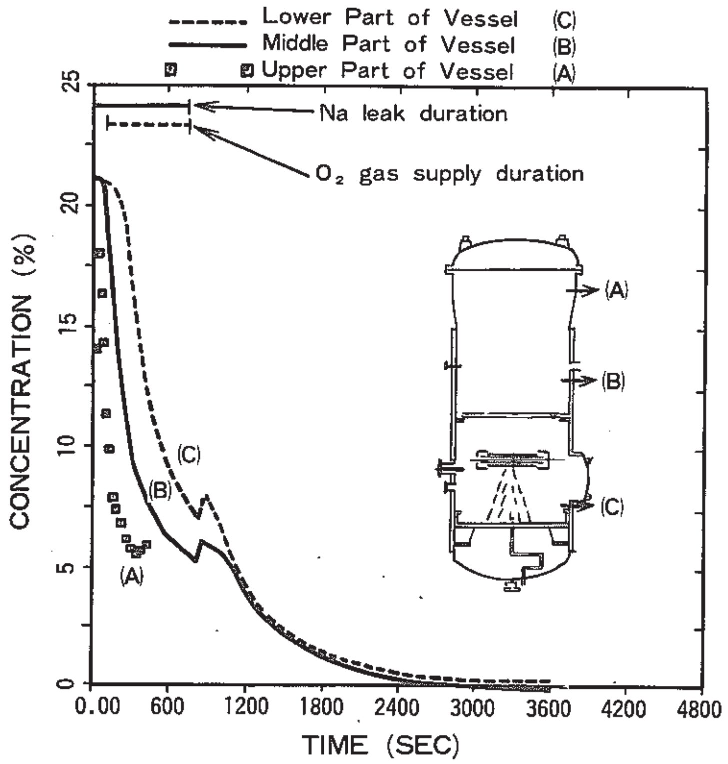

Fig. 4.8 Transient Oxygen Concentration

(PSS-SFE-534)

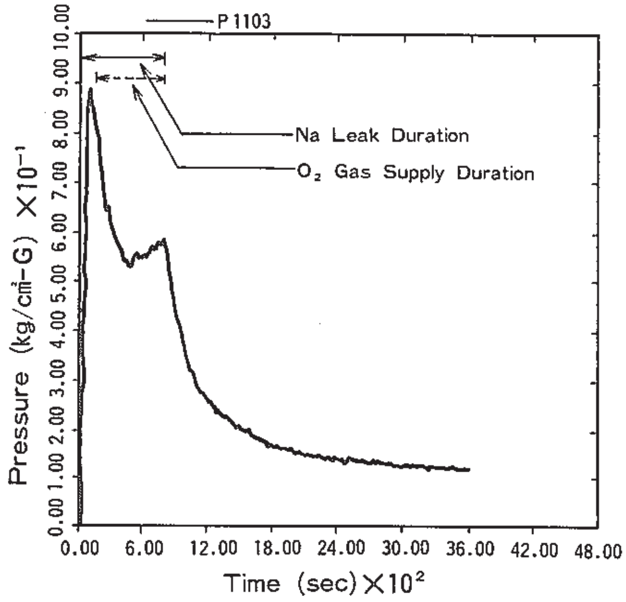

Fig. 4.9 Transient Gas Pressure

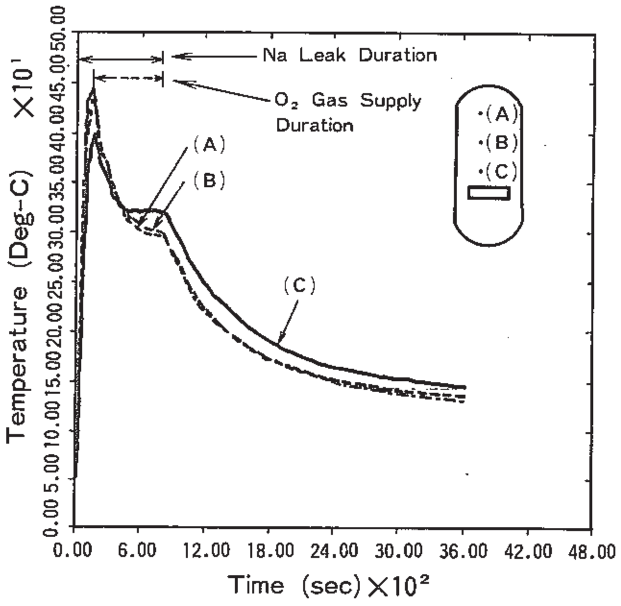

Fig. 4.10 Transient Gas Temperature above Test Pipe

(PSS - SFE - 398)

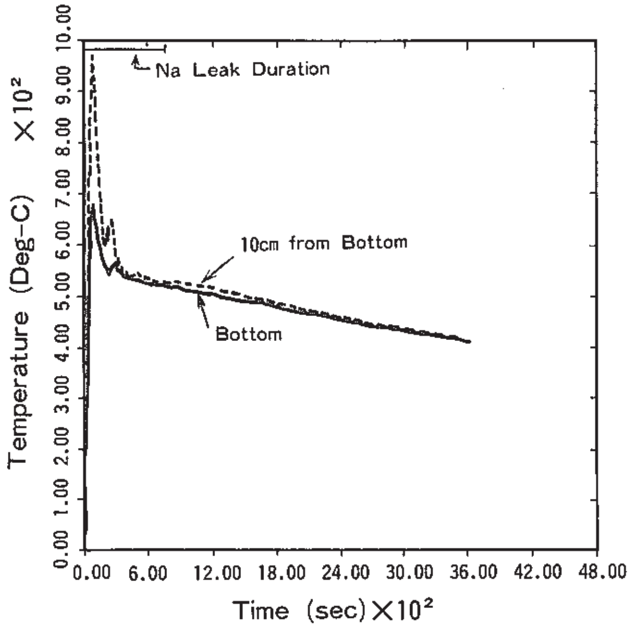

Fig. 4.11 Transient Pool Temperatures

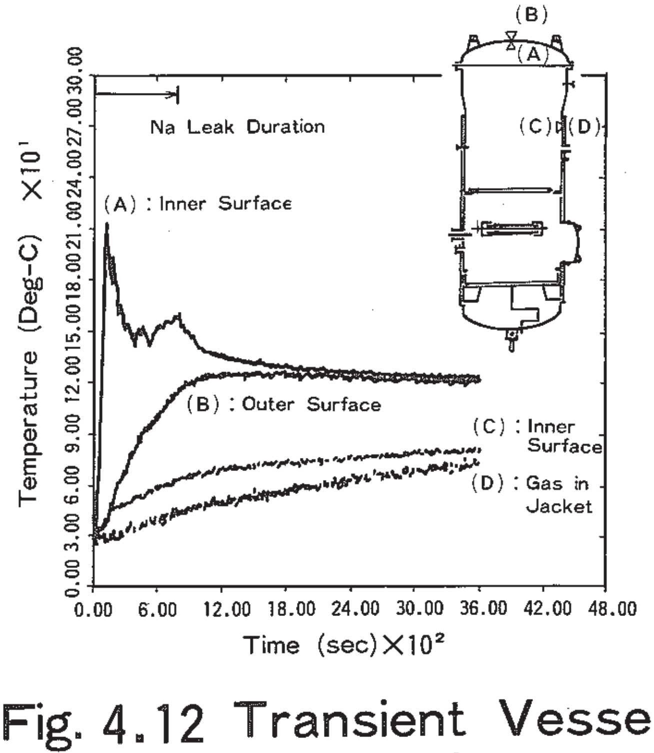

Fig. 4.12 Transient Vessel Temperatures

(PSS - SFE - 399)

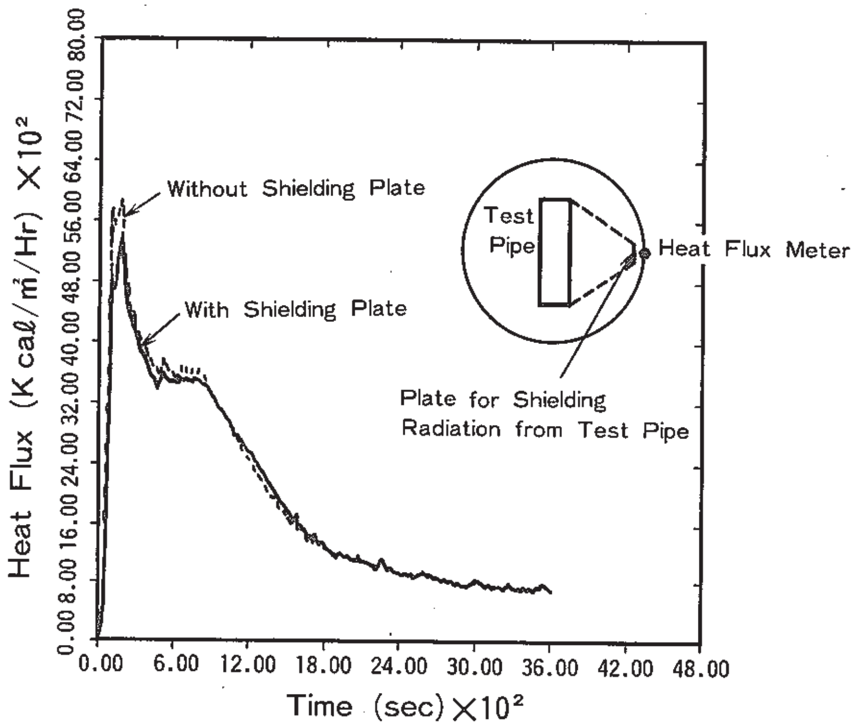

Fig. 4.13 Transient Heat Flux Toward Vessel Wall

(PSS - SFE - 400)

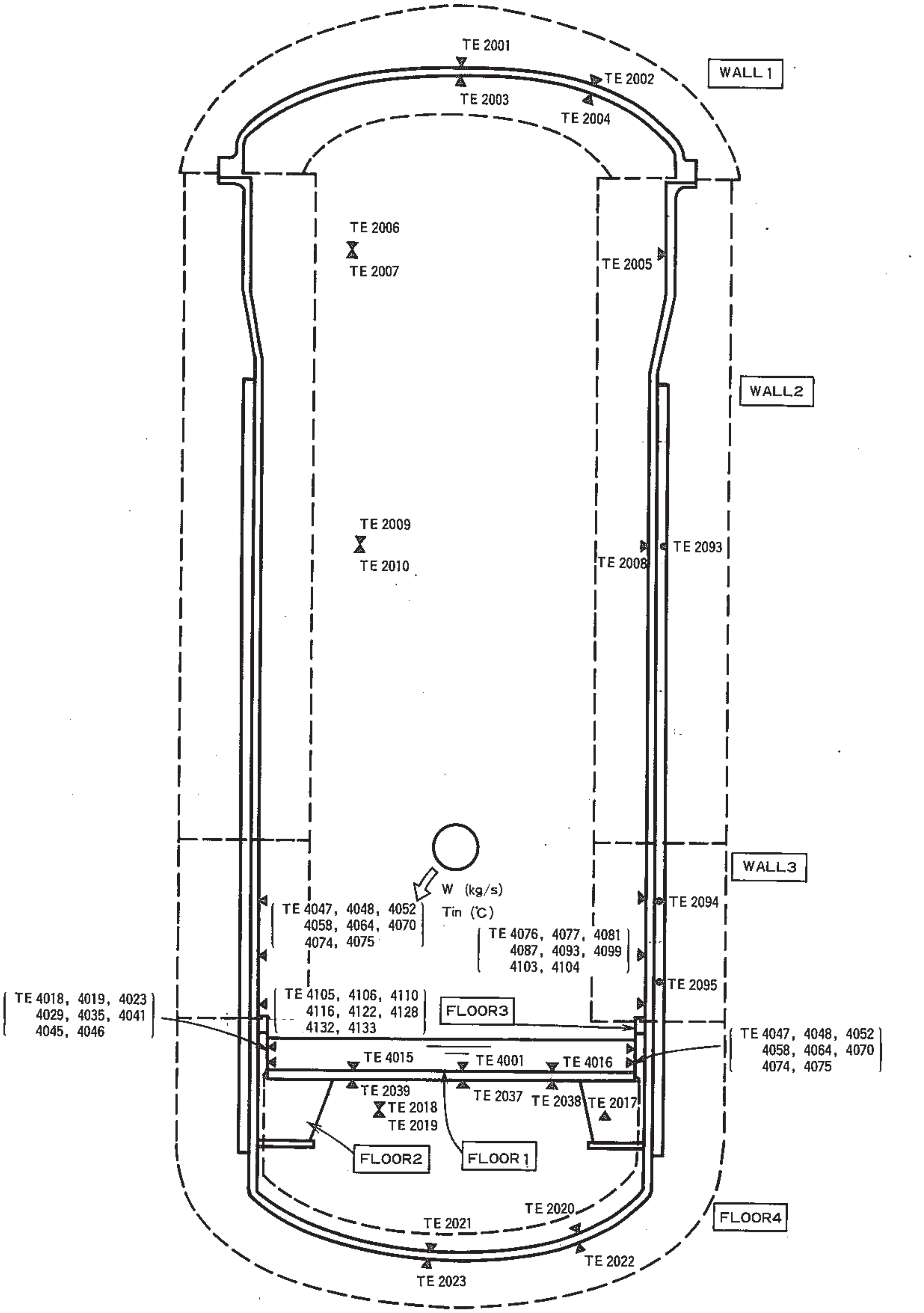

Fig. 4.14 Partition of Structures of Test Vessel for Evaluating Energy Balance

(PSS-SFE-531)

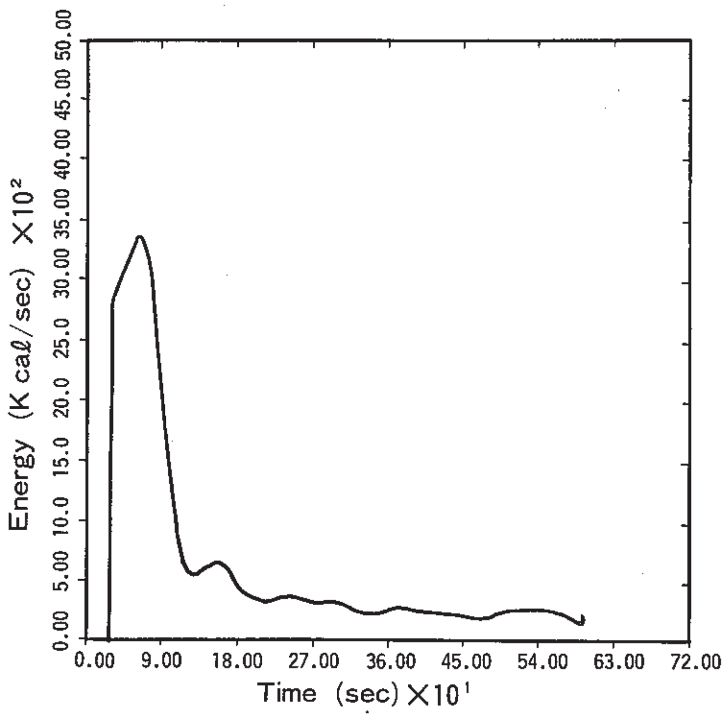

Fig. 4.15 Total Combustion Energy

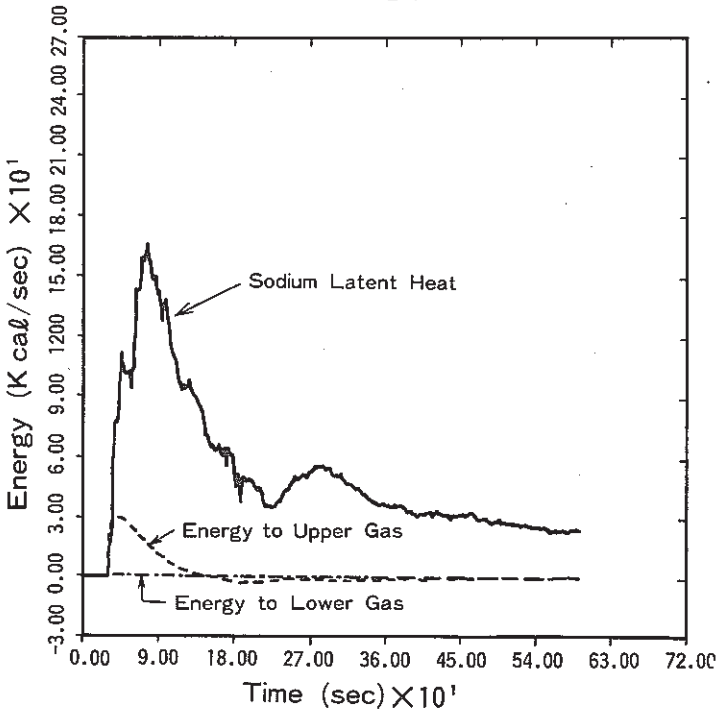

Fig. 4.16 Sodium Latent Heat and Energy Transfered to Gas

(PSS - SFE - 401)

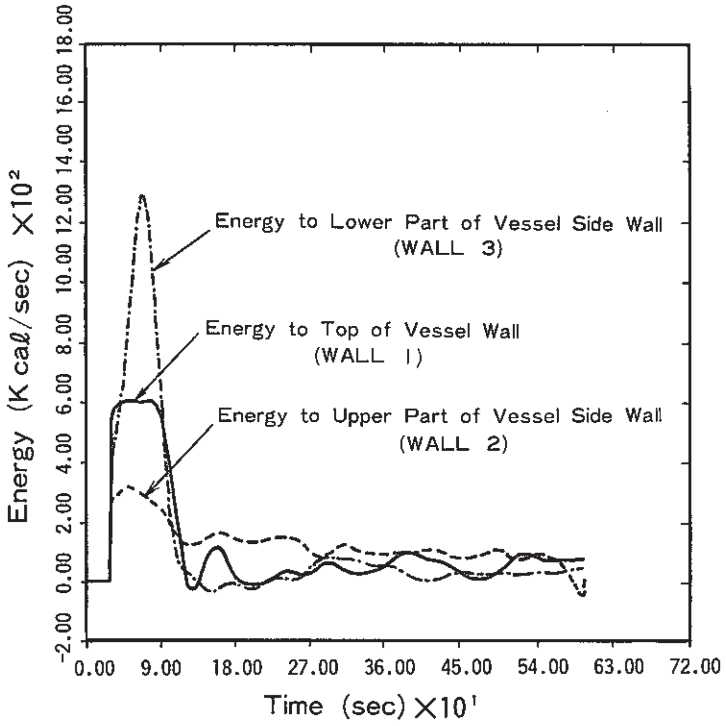

Fig. 4.17 Energy to Vessel Wall

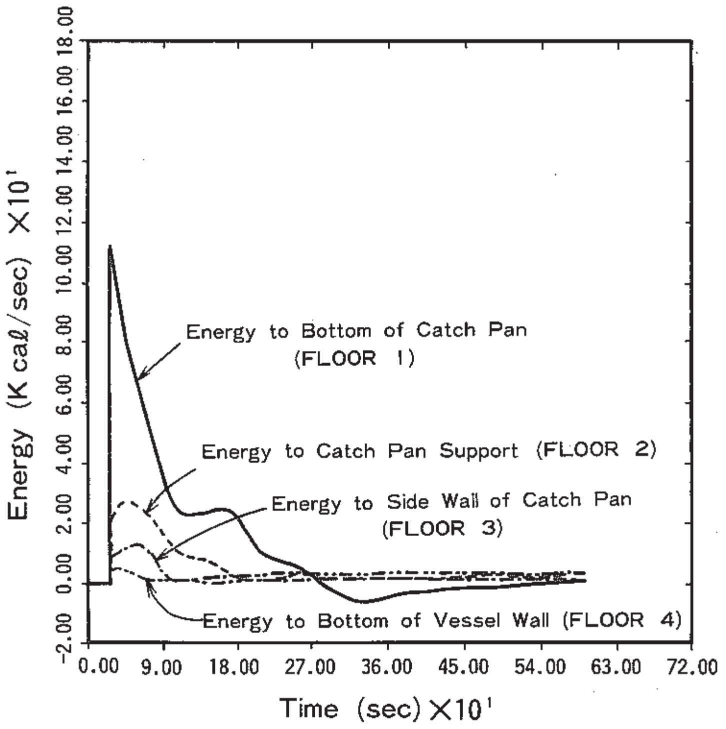

Fig. 4.18 Energy to Catch Pan

(PSS - SFE - 402)

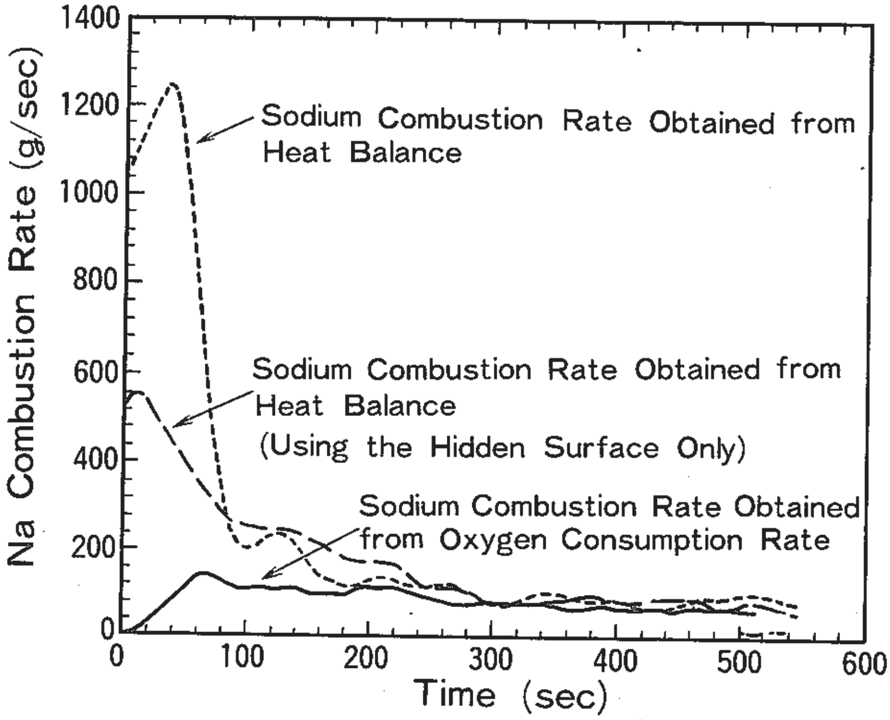

Fig. 4.19 Sodium Combustion Rate

(PSS - SFE - 403)

Appendix :

Gas Temperature Profiles

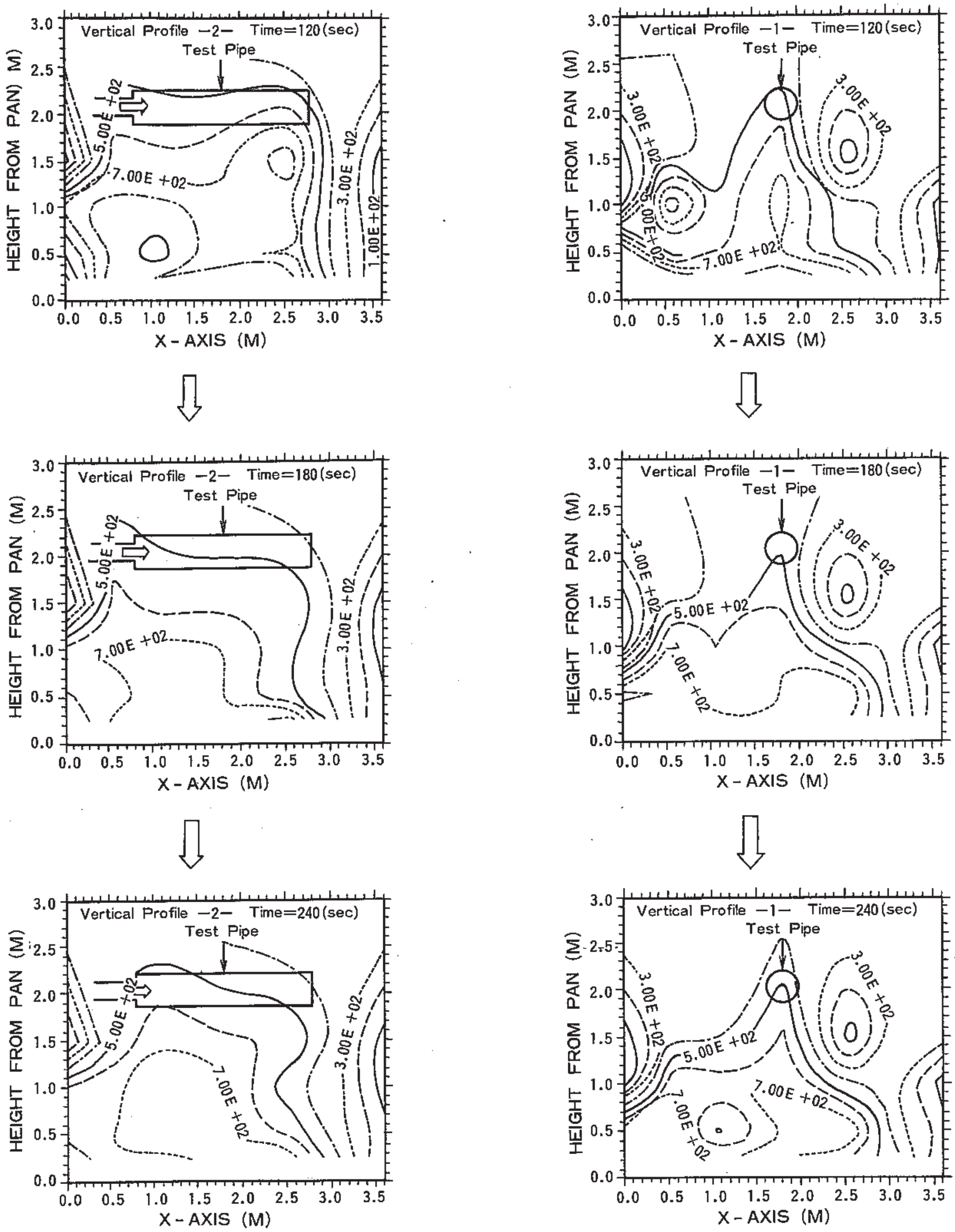

Fig. A. 1 Temperature Profiles of Gas Phase below Test Pipe (Vertical Profiles) 120 sec~240 sec (PSS-SFE-532)

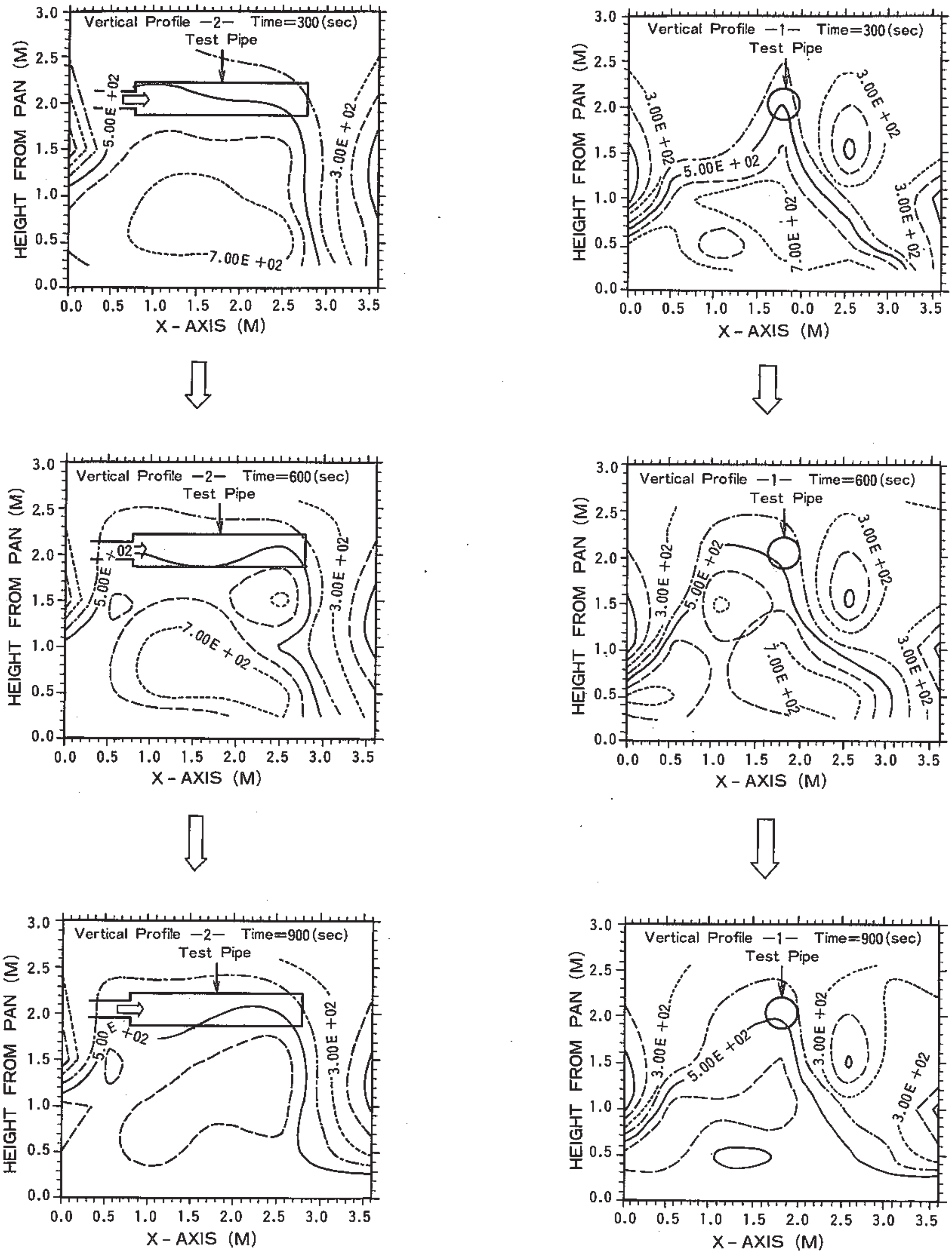

Fig. A. 2 Temperature Profiles of Gas Phase below Test Pipe (Vertical Profiles) 300 sec~900 sec

(PSS-SFE-533)